Diagnosing the loss of EPs and causes

M. Garcia-Munoz

University of Seville

Synthetic ITER FILD measurement:
Alpha particles losses induced by n=4 RMP

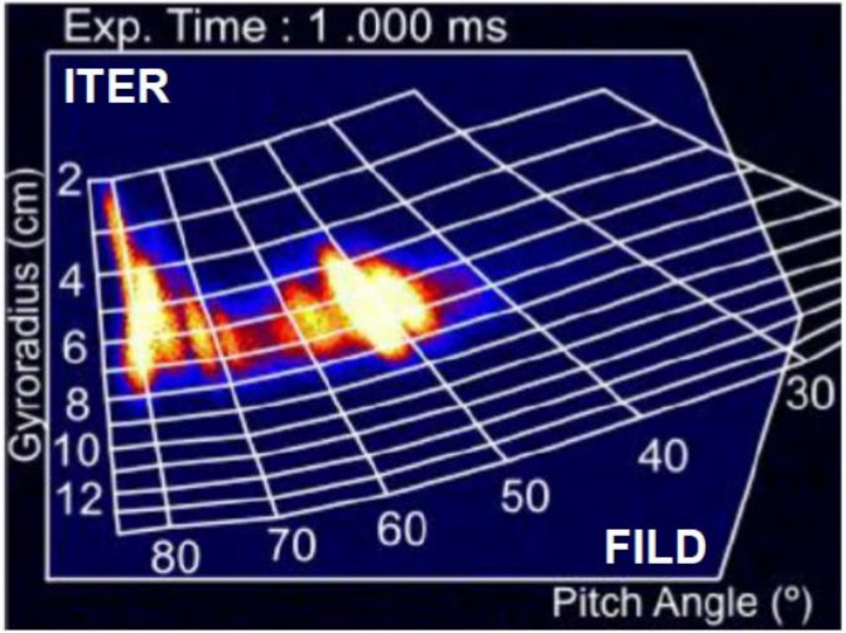

M. Garcia-Munoz *et al.,* Rev. Sci. Instrum. **87**, 11D829 (2016)

Outline

- Requirements of a Fast-Ion Loss Detector
- Scintillator-based Fast-Ion Loss Detector (FILD)
- Fast-Ion Losses Induced by:
  - Alfven Eigenmodes
  - Externally Applied Resonant Magnetic Perturbations
  - Edge Localized Modes (ELMs)
- Radial Profiles of Fast-Ion Losses
- Synthetic FILD (FILDSIM)

Outline

- **Requirements of a Fast-Ion Loss Detector**
- Scintillator-based Fast-Ion Loss Detector (FILD)
- Fast-Ion Losses Induced by:
  - Alfven Eigenmodes
  - Externally Applied Resonant Magnetic Perturbations
  - Edge Localized Modes (ELMs)
- Radial Profiles of Fast-Ion Losses
- Synthetic FILD (FILDSIM)

Particle Confinement is Ensured in Quiescent Axisymmetric Tokamaks

- Constants of motion (E, μ, P_{Φ}) are conserved

- Perturbations break constants of motion

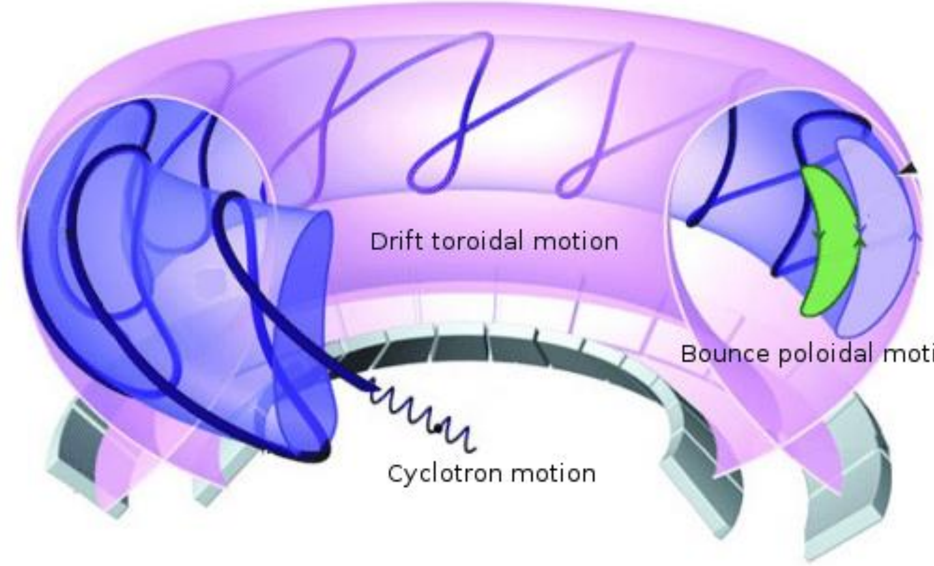

Particle Confinement is Ensured in Quiescent Axisymmetric Tokamaks

- Constants of motion **(E, μ, P_Φ)** are conserved

- Perturbations break constants of motion

  - **$\mu \neq$ const** if
    - $\Omega_c\, \delta_t \sim 1$, $\rho \dfrac{\nabla B}{B} \sim 1$

RF Heating Mechanism

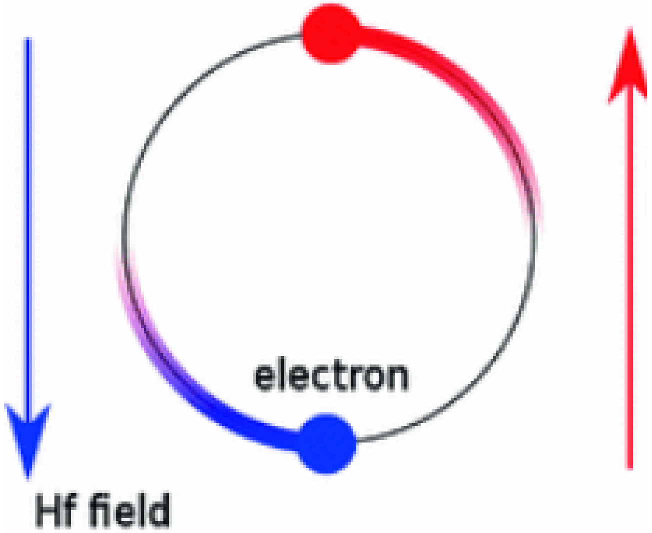

Particle Confinement is Ensured in Quiescent Axisymmetric Tokamaks

- Constants of motion **(E, μ, P_Φ)** are conserved

- Perturbations break constants of motion

  - ➢ **μ ≠ const** if
    - $\Omega_c\, \delta_t \sim 1$, $\rho \frac{\nabla B}{B} \sim 1$

  - ➢ **P_Φ ≠ const** in presence of symmetry breaking 3D fields

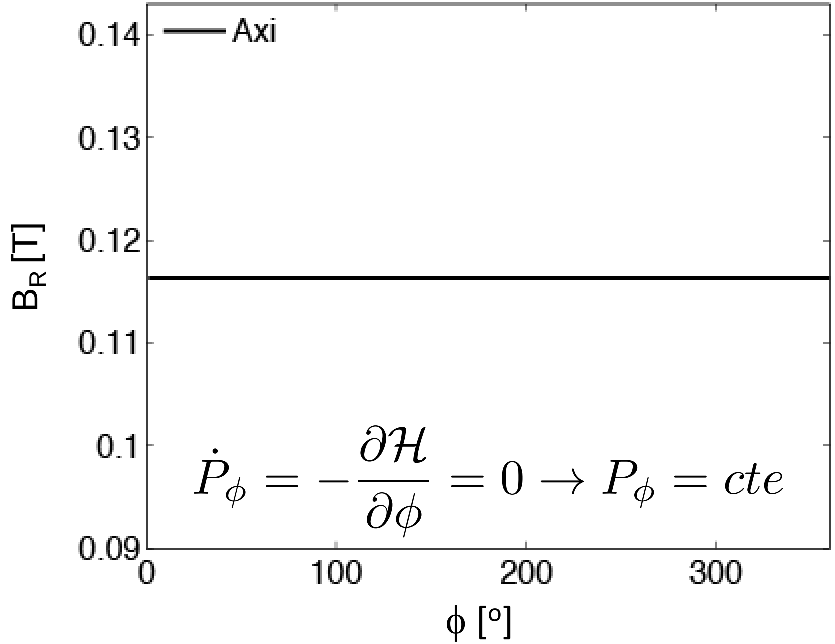

Particle Confinement is Ensured in Quiescent Axisymmetric Tokamaks

- Constants of motion **(E, μ, P_Φ)** are conserved

- Perturbations break constants of motion

  - **μ ≠ const** if
    - $\Omega_c\, \delta_t \sim 1\ ,\ \ \rho \dfrac{\nabla B}{B} \sim 1$

  - **P_Φ ≠ const** in presence of symmetry breaking 3D fields

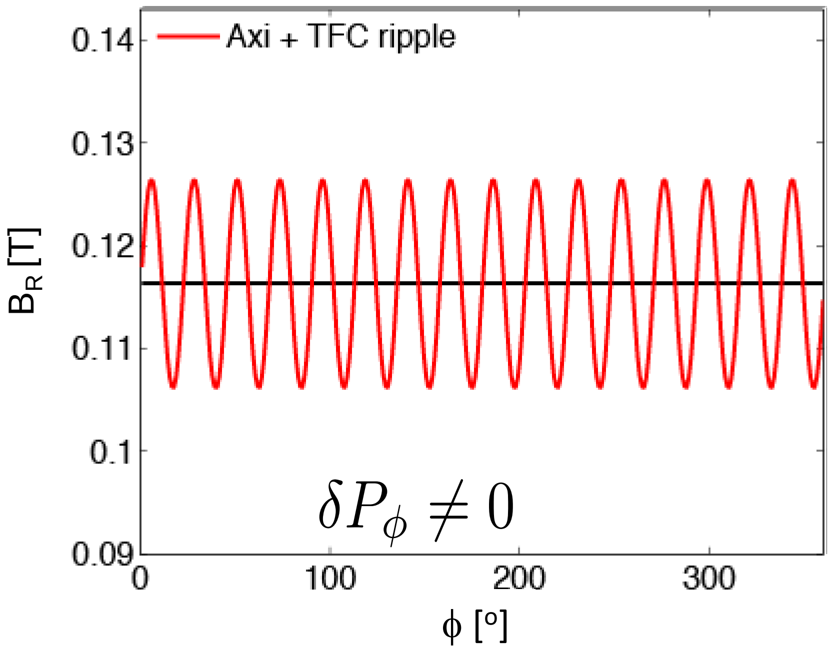

Particle Confinement is Ensured in Quiescent Axisymmetric Tokamaks

- Constants of motion **(E, μ, P_Φ)** are conserved

- Perturbations break constants of motion

  - **μ ≠ const** if
    - $\Omega_c\,\delta_t \sim 1$, $\rho \dfrac{\nabla B}{B} \sim 1$

  - **P_Φ ≠ const** in presence of symmetry breaking 3D fields

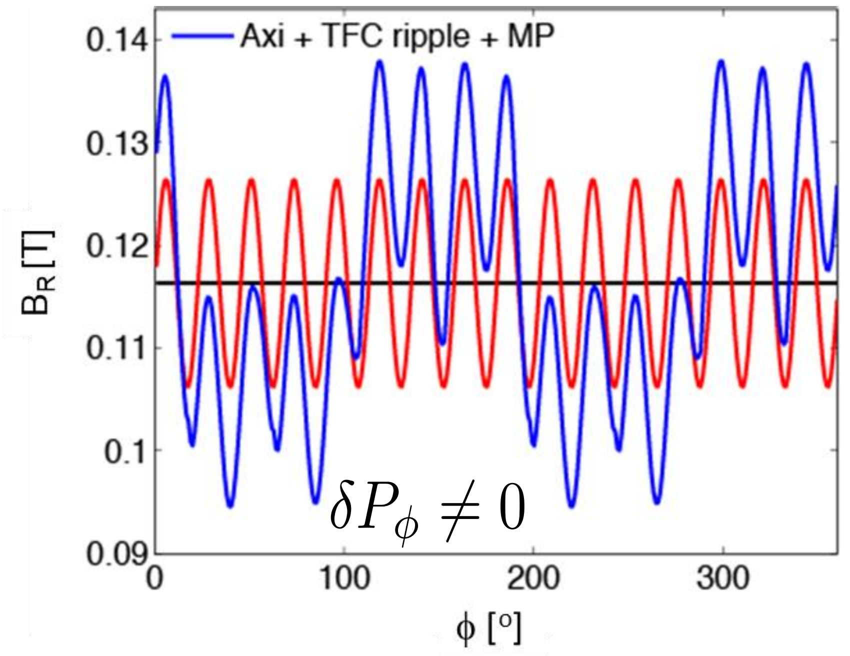

Orbit Poloidal Projections Are Not Close in Presence of Perturbations

- Variation in P_ϕ produces a radial drift

$$\boxed{P_\phi = mRv_\phi - Ze\psi}$$

$$\delta P_\phi \neq 0 \begin{cases} \delta P_\phi < 0 & \text{Outward orbit drift} \\ \delta P_\phi > 0 & \text{Inward orbit drift} \end{cases}$$

- Large / resonant perturbations lead to large drifts / losses

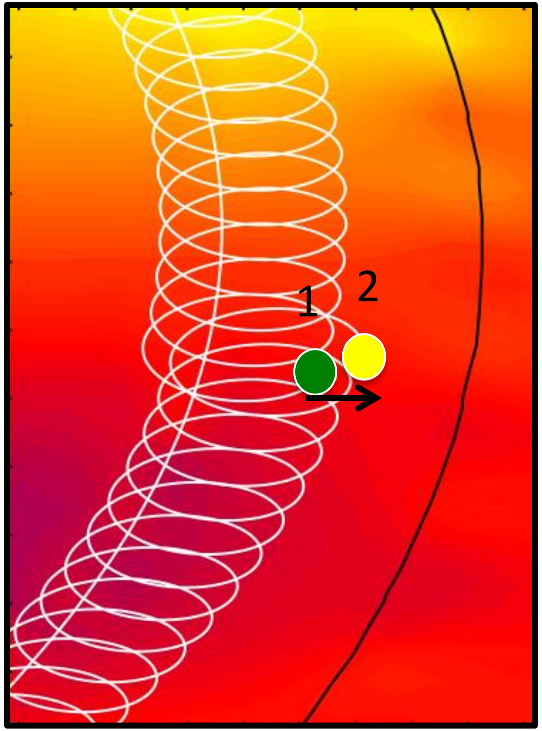

$\delta P_\phi > 0$ $\quad$ $\delta P_\phi < 0$

Small 3D Perturbations Can Lead to Large Resonant Particle Transport

- Externally applied static 3D fields are excellent control tools to test models
  - Routinely used to control internal MHD fluctuations and, more recently, fast-ion distributions

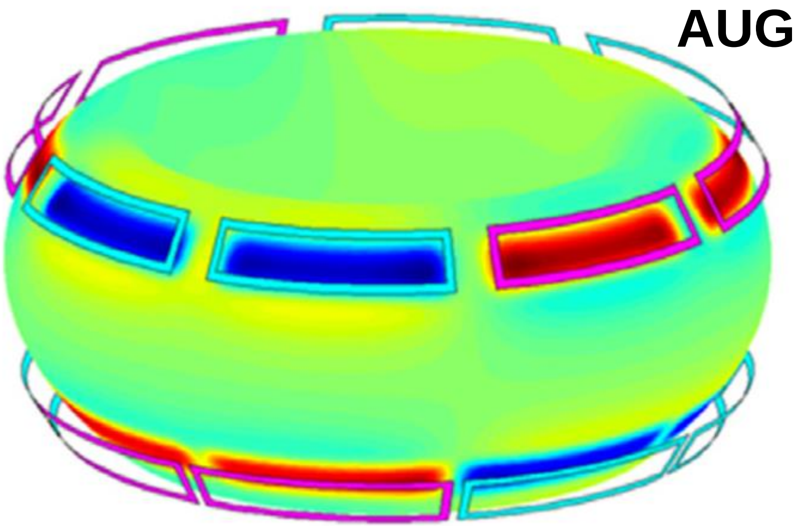

Small 3D Perturbations Can Lead to Large Resonant Particle Transport

- Externally applied static 3D fields are excellent control tools to test models
  - Routinely used to control internal MHD fluctuations and, more recently, fast-ion distributions

AUG

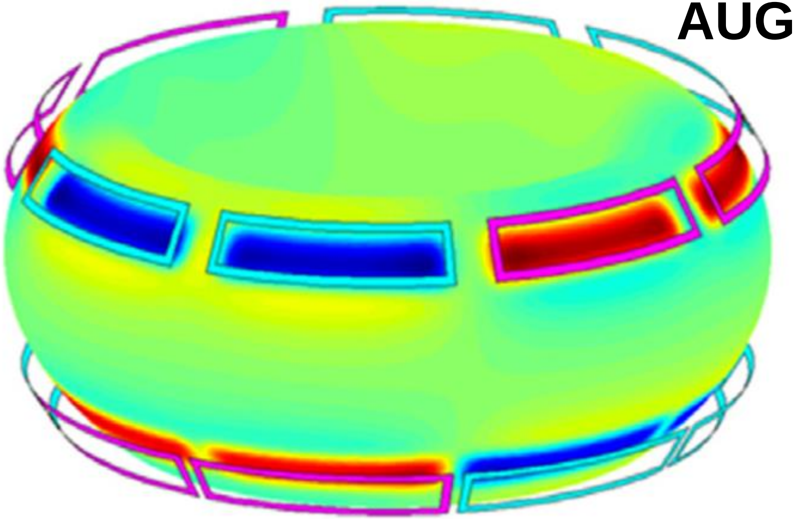

Small 3D Perturbations Can Lead to Large Resonant Particle Transport

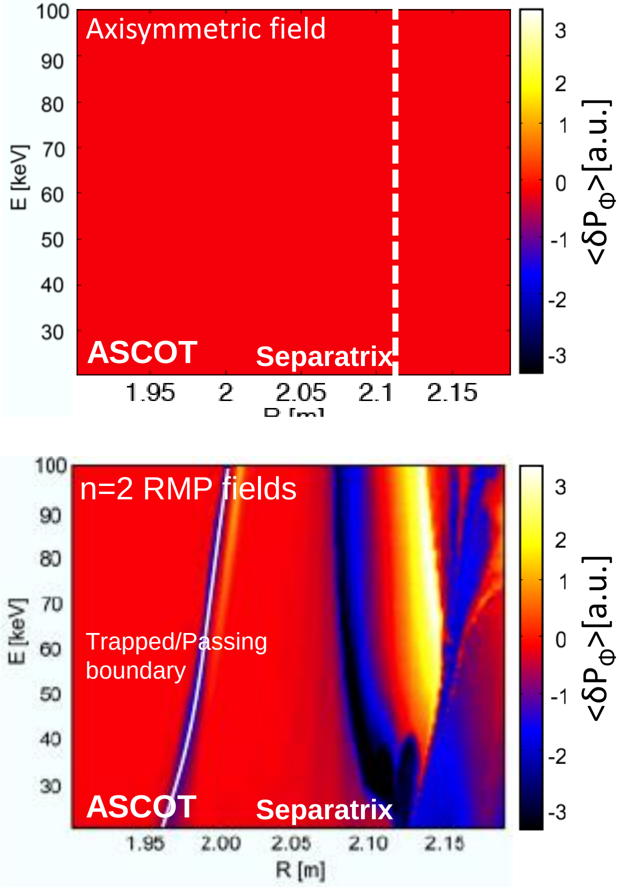

- Orbit following codes are used to identify transport mechanisms
  - <δP_Φ> figure of merit calculated by averaging δP_Φ over time with particles started with same z, phi and pitch
  - n=2 3D fields w/o plasma response

L. Sanchis-Sanchez *et al.*, PPCF 61 014038 (2019)

Combination of Multiple Linear / Non-Linear Resonances Creates an Edge Resonance Transport Layer (ERTL)

- **Orbital resonances intrinsic to magnetic background**

$$\frac{\omega_b}{\bar{\omega}_d} = \frac{n(l+1)}{p_0(l+1) \pm p'}$$

  - n: toroidal mode number
  - l: nonlinear harmonic
  - p_0: main bounce harmonic
  - p': nonlinear bounce harmonic

- Maximum transport caused by a combination of resonances

- Non-linear resonances seem to play a key role

[*]

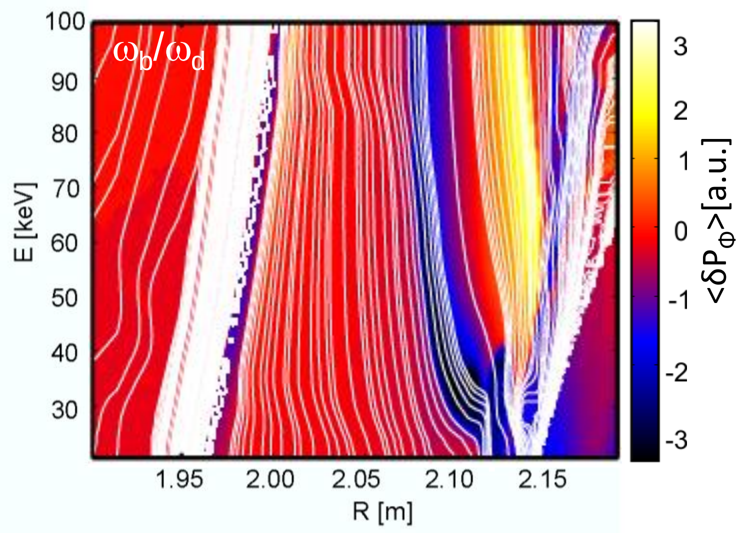

$<\delta P_\Phi> < 0$ (blue-black) → **outwards transport**

$<\delta P_\Phi> > 0$ (yellow-white) → **inwards transport**

L. Sanchis-Sanchez *et al.*, PPCF 61 014038 (2019)

[*] F .Zonca et al, NJP 17 (2015)0130052

Combination of Multiple Linear / Non-Linear Resonances Creates an Edge Resonance Transport Layer (ERTL)

- **Orbital resonances intrinsic to magnetic background**

$$\frac{\omega_b}{\bar{\omega}_d} = \frac{n(l+1)}{p_0(l+1) \pm p'}$$

  - n: toroidal mode number
  - l: nonlinear harmonic
  - p_0: main bounce harmonic
  - p': nonlinear bounce harmonic

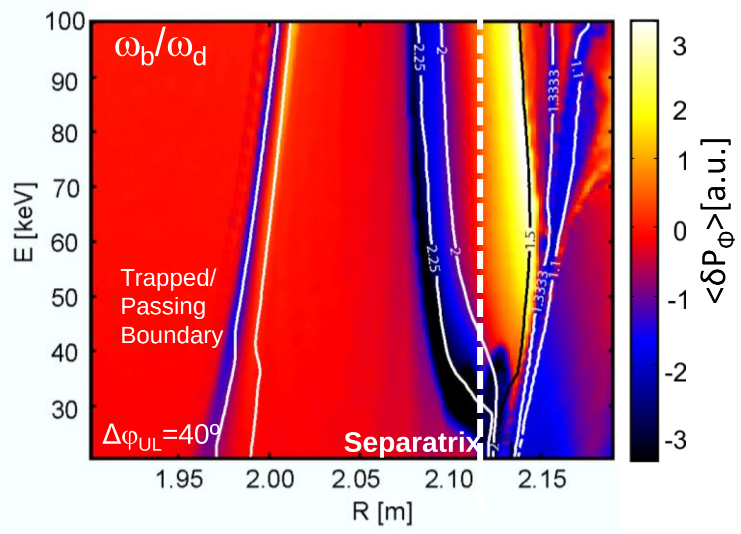

- Maximum transport caused by a combination of resonances

- Non-linear resonances seem to play a key role

$\langle \delta P_\Phi \rangle < 0$ (blue-black) → **outwards transport**

$\langle \delta P_\Phi \rangle > 0$ (yellow-white) → **inwards transport**

L. Sanchis-Sanchez *et al.*, PPCF 61 014038 (2019)

[*] F .Zonca et al, NJP 17 (2015)0130052

Fast-Ion Transport / Loss Mechanisms Given by Wave-Particle Interaction

Net wave-particle energy and momentum exchange achieved only if particle and wave are kept in phase long enough

- Resonance condition

$$\Omega_{\mathrm{n,p}} = n\omega_{\phi} - p\omega_{\theta} - \omega$$

ω=0 for (quasi)-static perturbations

- Orbital frequencies are given by fast-ions constants of motion

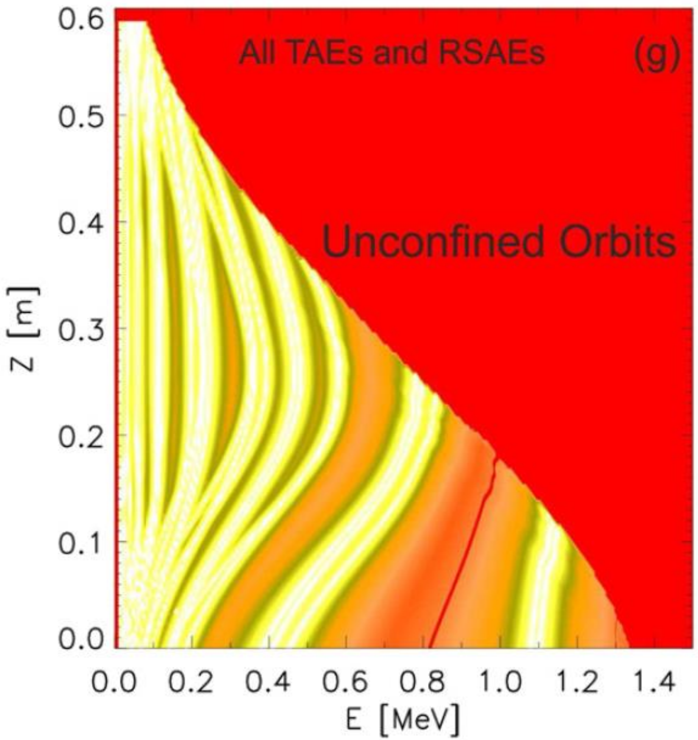

Loss ion orbit topology is key to identify loss mechanism

M. Garcia-Munoz *et al.*, NF **51** 103013 (2011)

Fast-Ion Transport / Loss Mechanisms Given by Wave-Particle Interaction

Net wave-particle energy and momentum exchange achieved only if particle and wave are kept in phase long enough

- Resonance condition

$$\Omega_{\mathrm{n,p}} = n\omega_{\phi} - p\omega_{\theta} - \omega$$

$\omega=0$ for (quasi)-static perturbations

- Orbital frequencies are given by fast-ions constants of motion

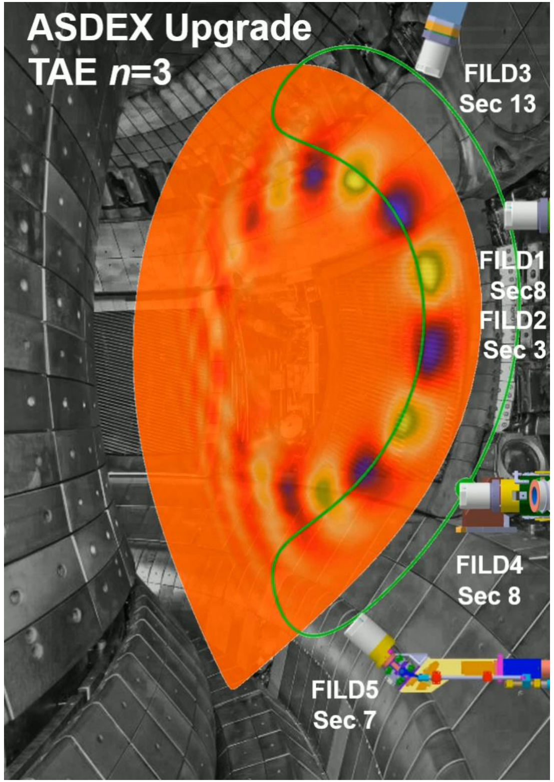

Loss ion orbit topology is key to identify loss mechanism

Fast-Ion Heat Loads Are Not Axisymmetric

Fast-ion loss mechanisms lead to complex 3D heat load patterns on vacuum vessel

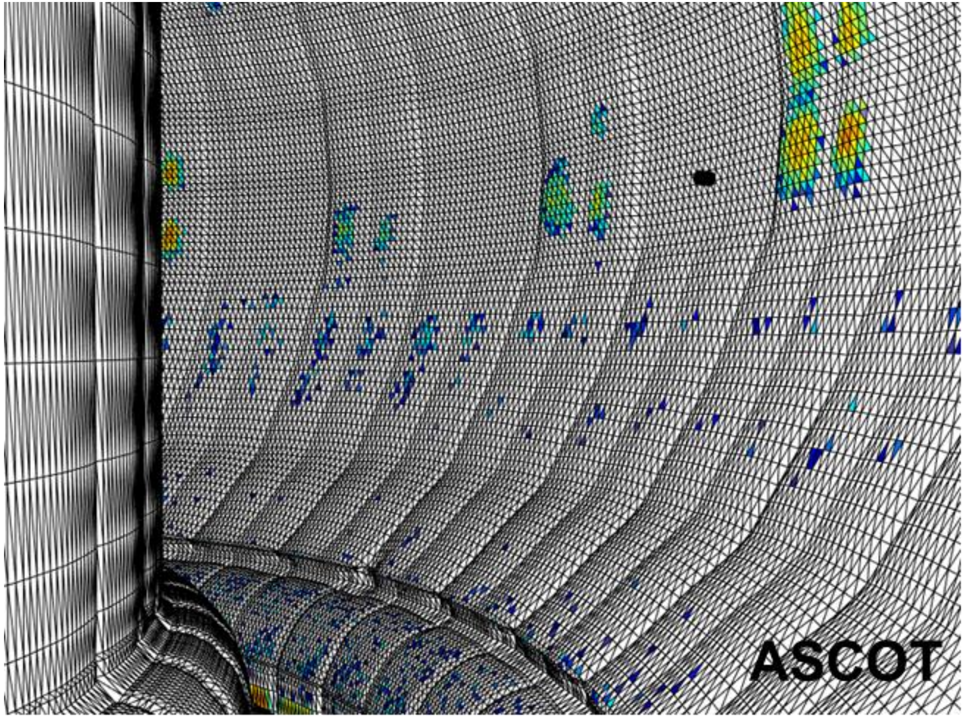

- Complex fast-ion distributions
  - Non axisymmetric, e.g. NBI deposition
  - Anysotropic, e.g. NBI and ICRH
- Perturbation spatio-temporal topology

Fast-Ion Heat Loads Are Not Axisymmetric

Fast-ion loss mechanisms lead to complex 3D heat load patterns on vacuum vessel

- Complex fast-ion distributions
  - Non axisymmetric, e.g. NBI deposition
  - Anysotropic, e.g. NBI and ICRH

- Perturbation spatio-temporal topology

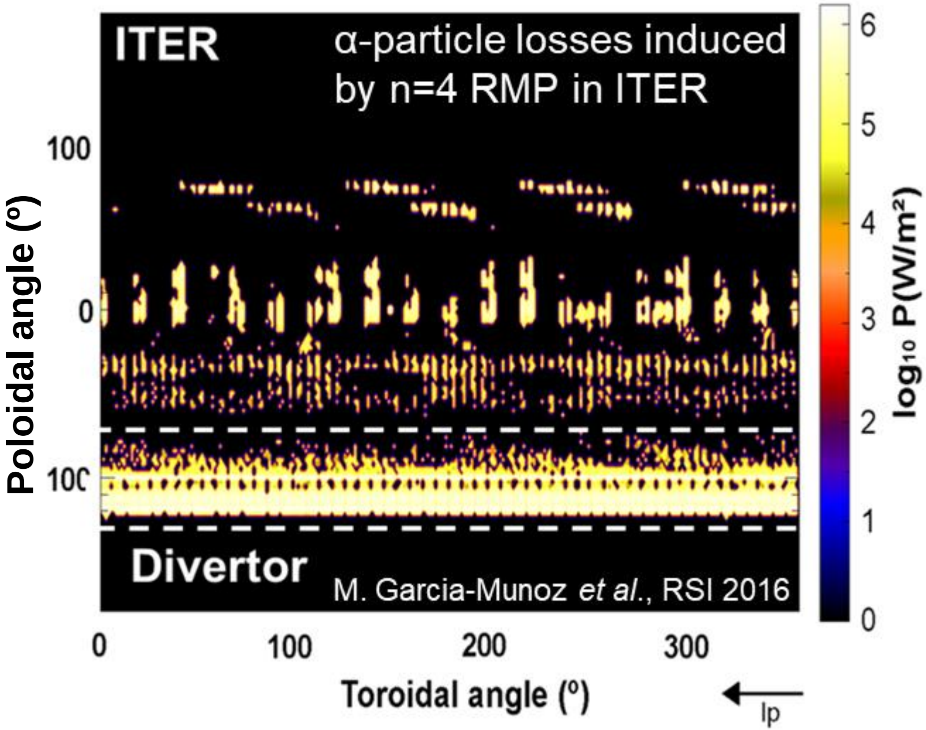

M. Garcia-Munoz *et al.,* Rev. Sci. Instrum. **87**, 11D829 (2016)

MHD Induced Fast-Ion Losses Can Damage Vacuum Vessel Components

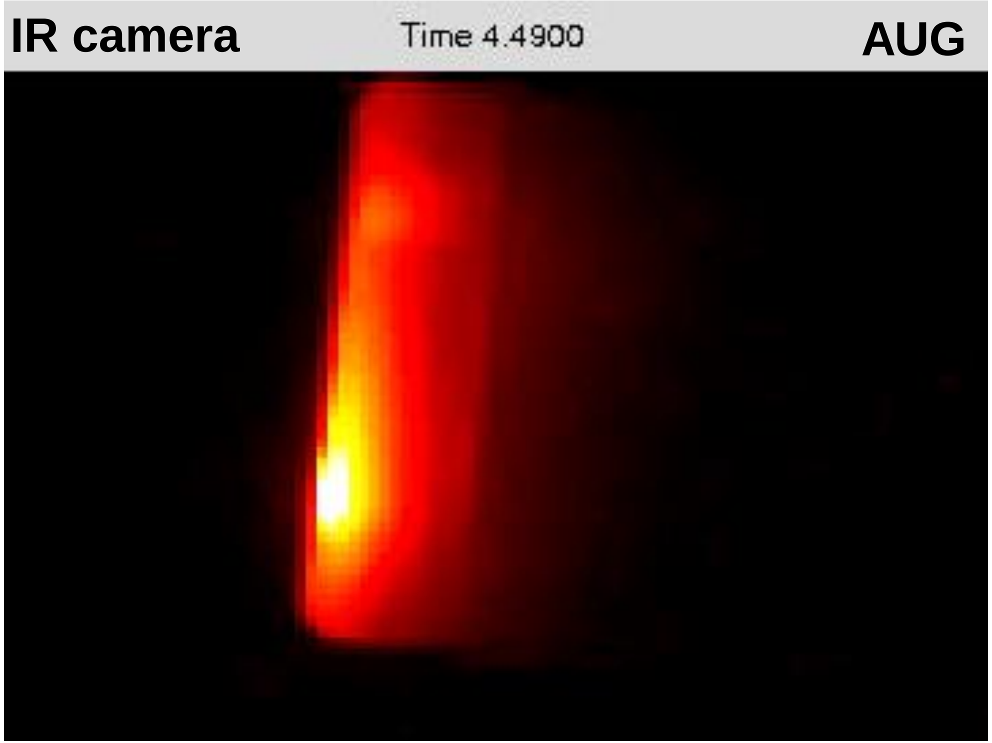

J. Galdon-Quiroga *et al* 2018 *Nucl. Fusion* **58** 036005

MHD Induced Fast-Ion Losses Can Damage Vacuum Vessel Components

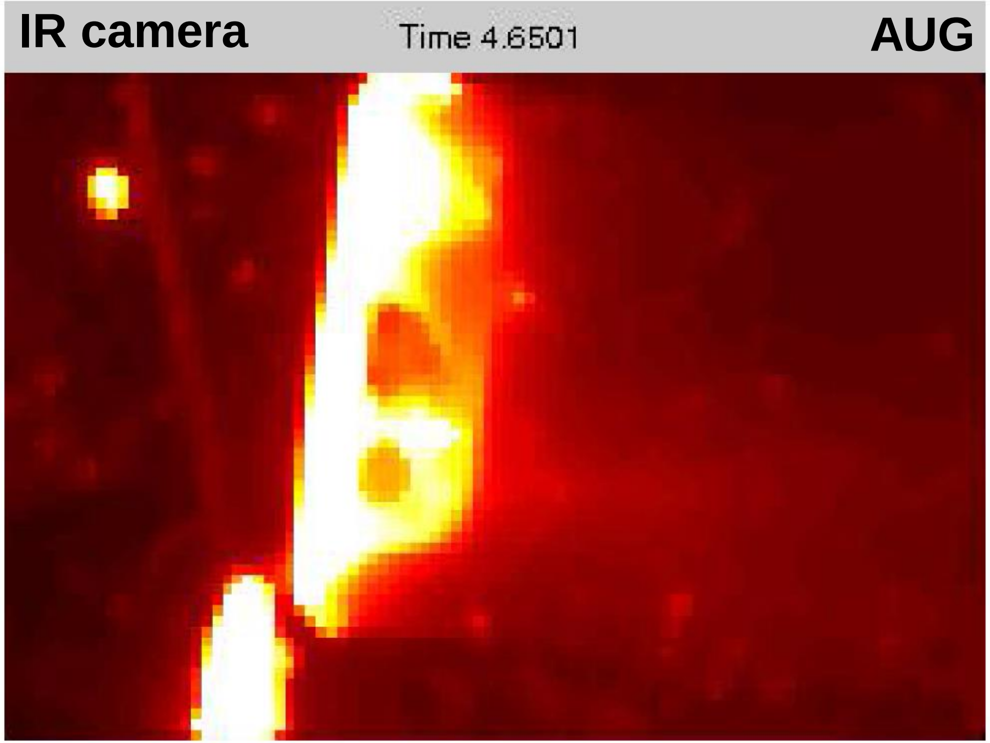

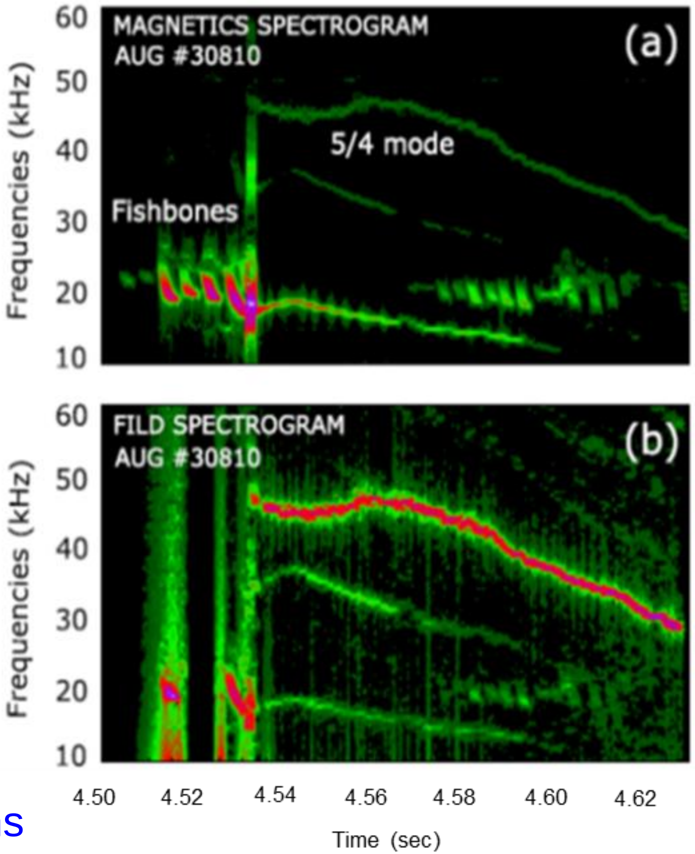

MHz temporal resolution is key to identify MHD fluctuations

J. Galdon-Quiroga *et al* 2018 *Nucl. Fusion* **58** 036005

Ideal Fast-Ion Loss Detector Covers Entire Phase-Space Volume of Escaping / Lost Ions

Ideal

- **Full 3D wall coverage**
- **Velocity-space information**
- **MHz temporal resolution**
- **Absolute flux**

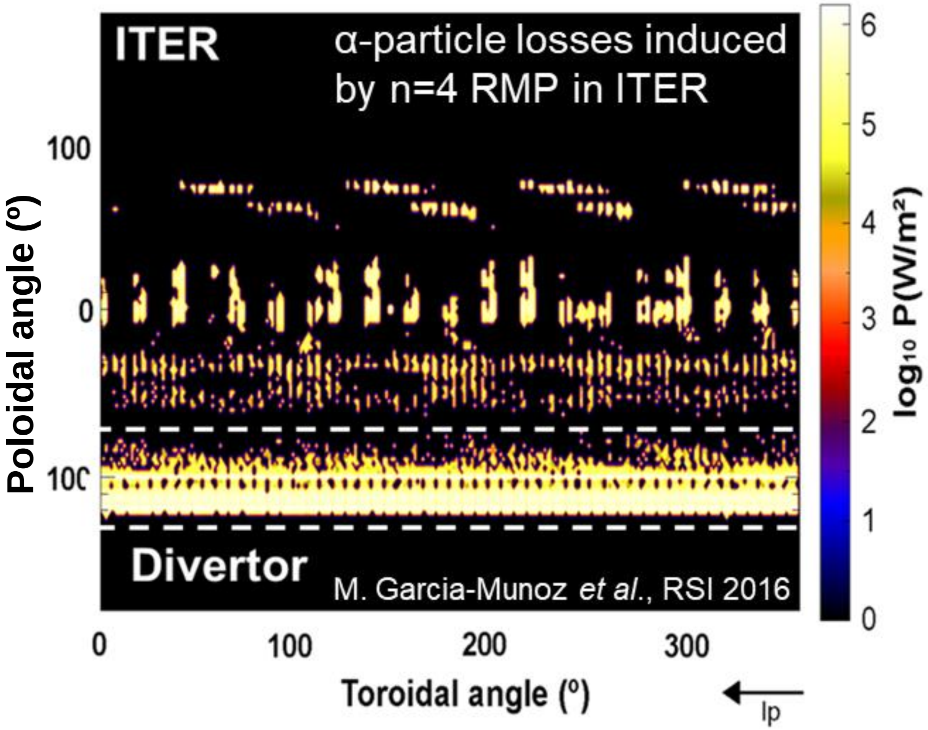

Ideal Fast-Ion Loss Detector Covers Entire Phase-Space Volume of Escaping / Lost Ions

Ideal

- Full 3D wall coverage
- Velocity-space information
- MHz temporal resolution
- Absolute flux

Affordable in present devices

- IR / VIS cameras for full coverage
- Charged particle collectors
- Indirect measurements of confined populations, e.g. neutron deficits

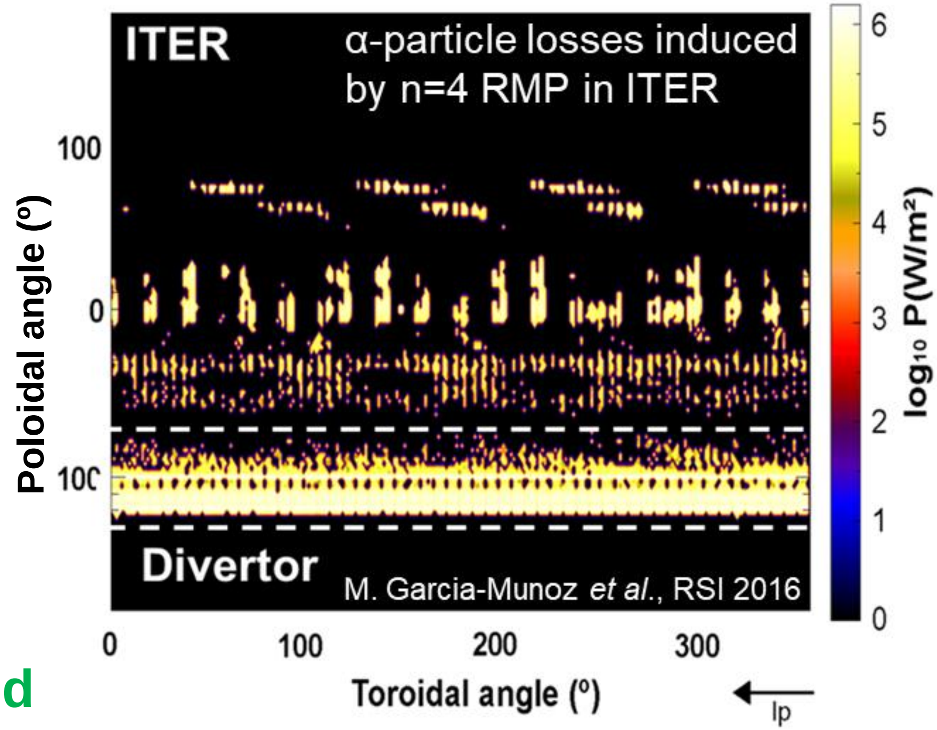

IR / VIS Cameras are Best Monitors for Safe Operation

Full coverage of 3D wall can be “easily” obtained with set of IR / VIS cams

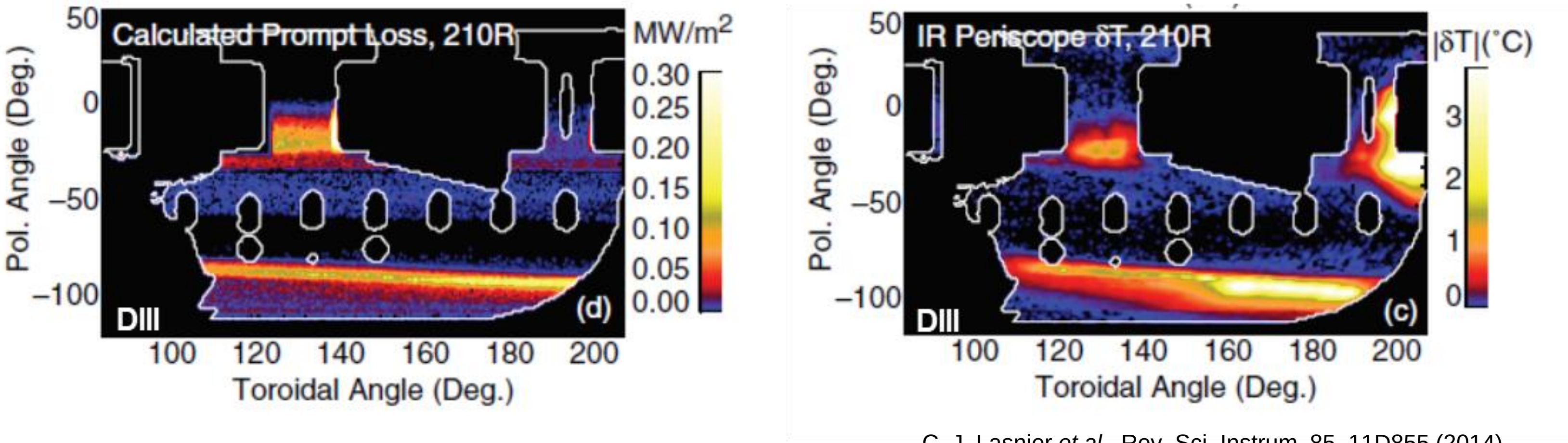

C. J. Lasnier *et al.,* Rev. Sci. Instrum. 85, 11D855 (2014)

IR / VIS Cameras are Best Monitors for Safe Operation

Full coverage of 3D wall can be "easily" obtained with set of IR / VIS cams

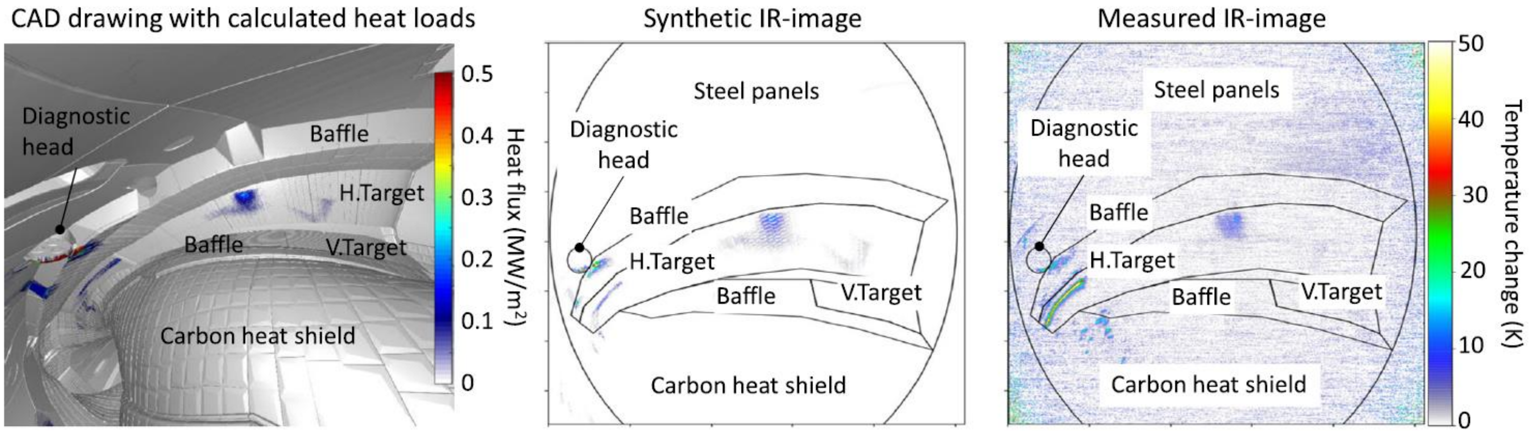

R. C. Wolf *et al*., Phys. Plasmas **26**, 082504 (2019)

IR / VIS Cameras are Best Monitors for Safe Operation

Full coverage of 3D wall can be “easily” obtained with set of IR / VIS cams

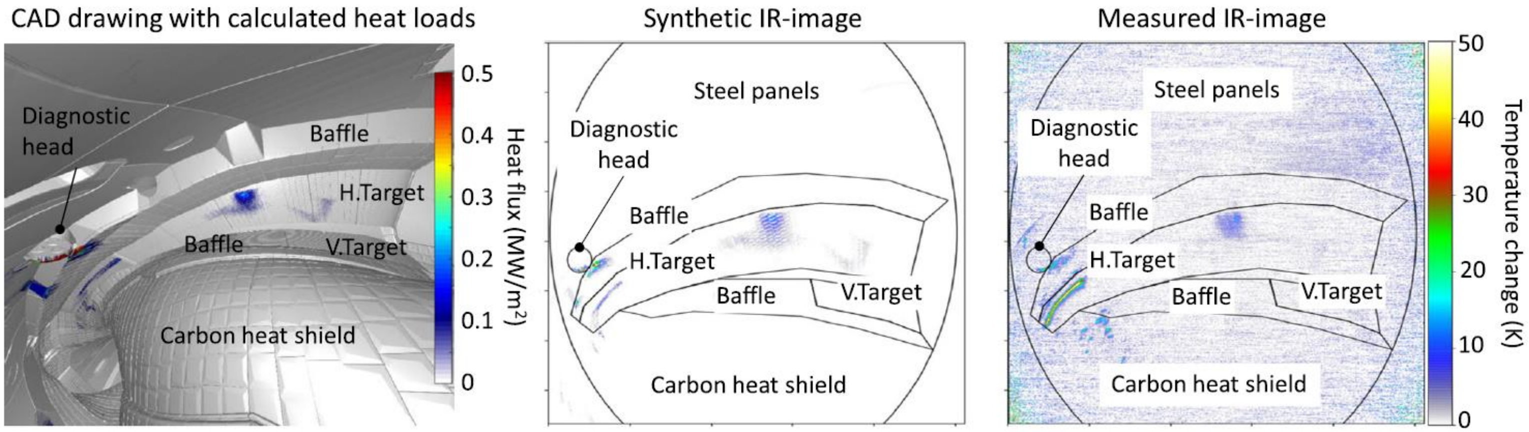

R. C. Wolf *et al.*, Phys. Plasmas **26**, 082504 (2019)

Caveats:

- Virtually impossible to distinguish **thermal** from **fast** particle loads without modelling
- **No velocity-space resolution**, i.e. identification of lost orbit topology
- **Limited temporal resolution**, i.e. identification of MHD fluctuations

Outline

- Requirements of a Fast-Ion Loss Detector
- **Scintillator-based Fast-Ion Loss Detector (FILD)**
- Fast-Ion Losses Induced by:
  - Alfven Eigenmodes
  - Externally Applied Resonant Magnetic Perturbations
  - Edge Localized Modes (ELMs)
- Radial Profiles of Fast-Ion Losses
- Synthetic FILD (FILDSIM)

Fast-Ion Loss Detector (FILD[1,2]) Provides Full Information on Velocity-Space of Escaping Ions

- FILD measures the pitch-angle and energy of lost fast ions
- Large bandwidth allows measurements at Alfvén Eigenmode frequencies (~100kHz) *– key for identifying coherent losses and impact of individual modes*
- Local velocity-space measurements like these help to isolate fundamental mechanisms
- Installed in virtually all fusion devices. Design for W7-X, JT-60SA and ITER on-going

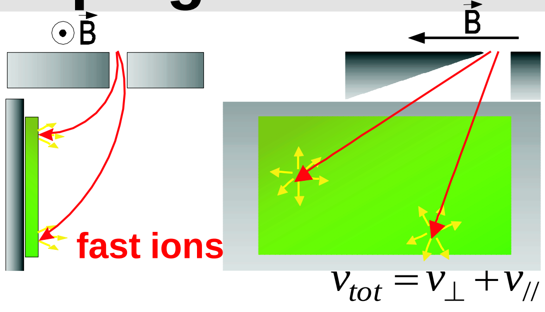

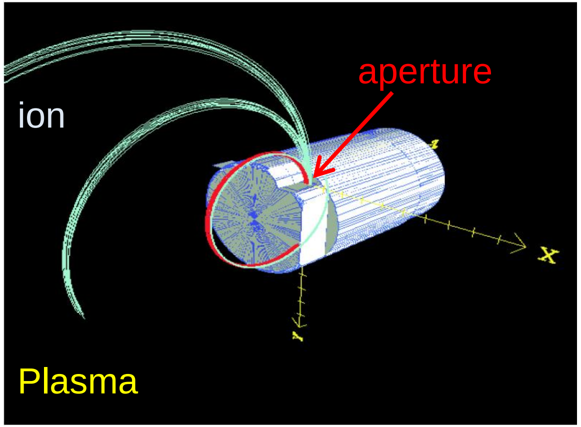

[1]S. J. Zweben, Rev. Sci. Instrum. **57**, 1774 (1986)

[2]M. Garcia-Munoz et al, Rev. Sci. Instrum. **80** 053003 (2009)

FILD Set-Up Overview

Simultaneous imaging of scintillator with double system

- CCD camera (slow but high spatial resolution)
- Array of 20 photomultiplier tubes (MHz - Alfvénic temporal resolution)

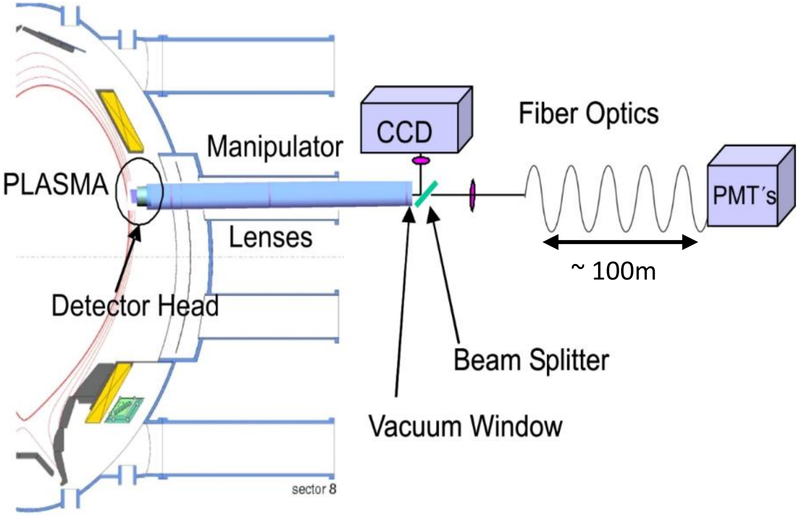

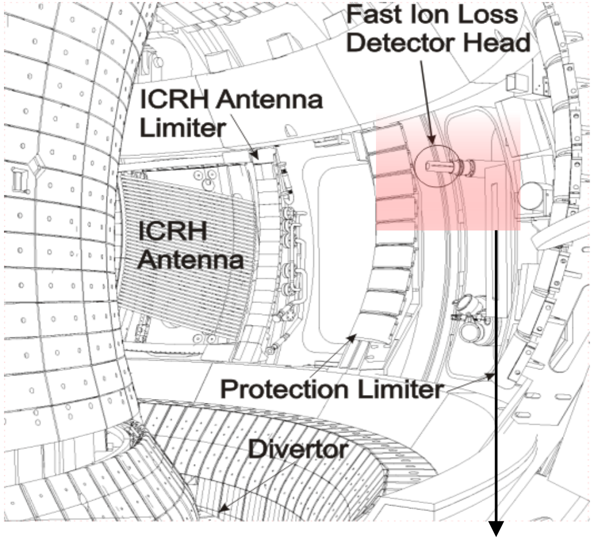

Safety & IR-Camera view

Fast-Ion Loss Detector (FILD[1,2]) Provides Full Information on Velocity-Space of Escaping Ions

Typical CCD Scintillator Image

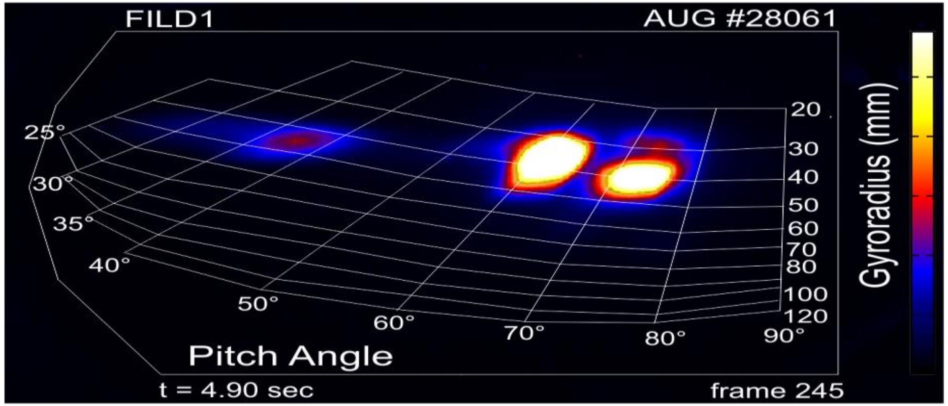

Identification of loss orbit topology

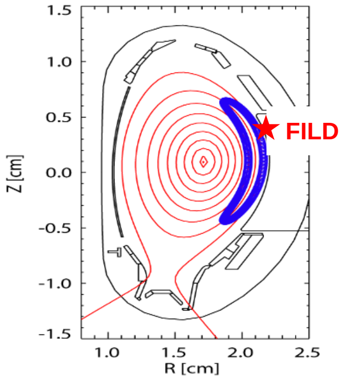

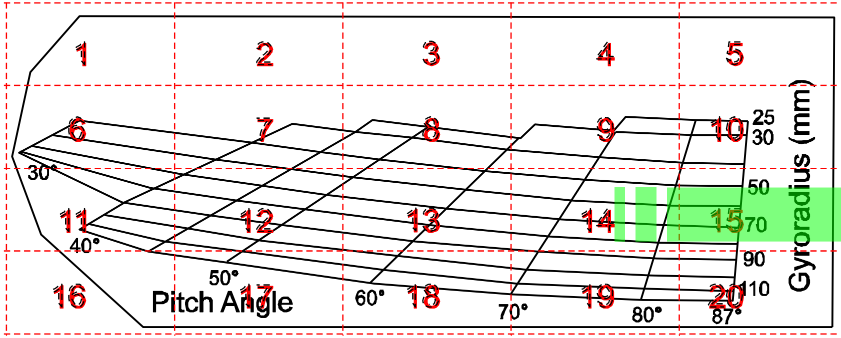

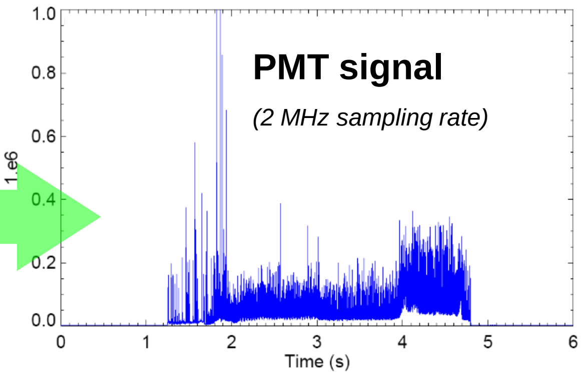

FILD Spectrogram Clearly Identifies MHD Fluctuations Responsible For Fast-Ion Losses

ASDEX Upgrade

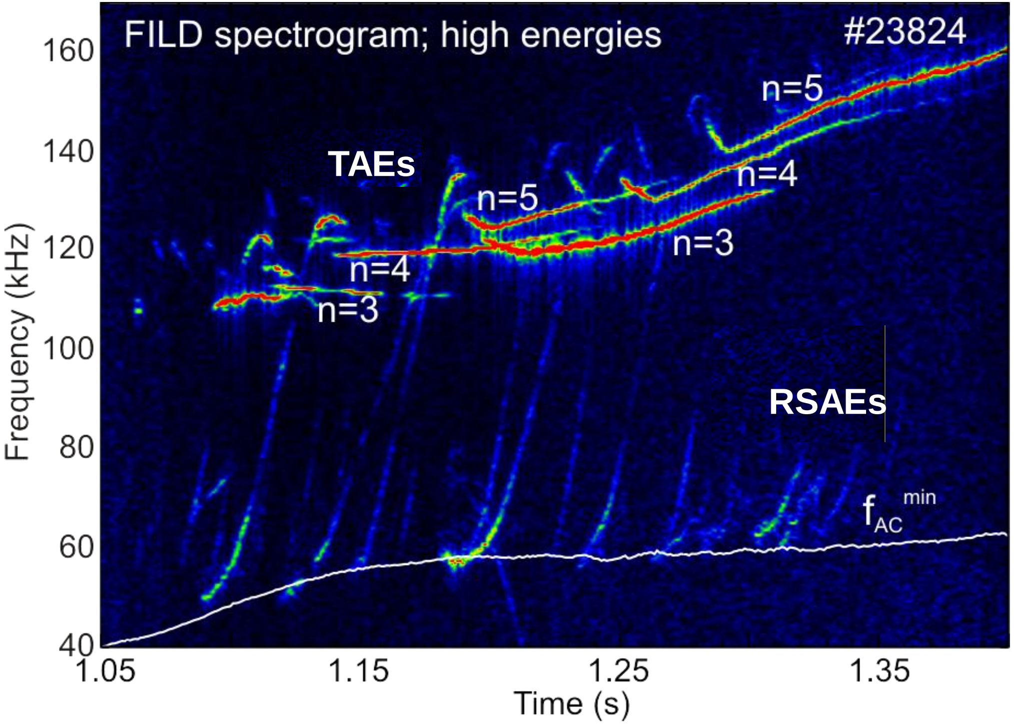

M. Garcia-Munoz et al, Phys. Rev. Lett. **104,** 185002 (2010)

Faraday Cup Measurement Embedded in Scintillator Plate

Secondary absolute measurements of fast-ion loss flux

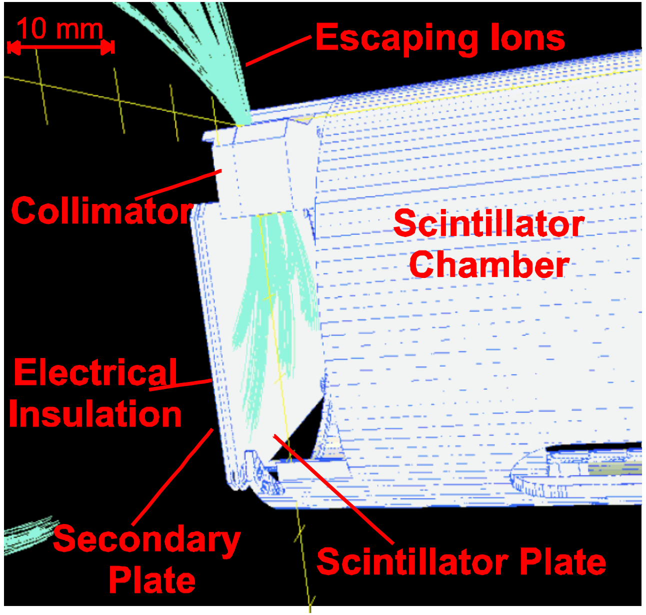

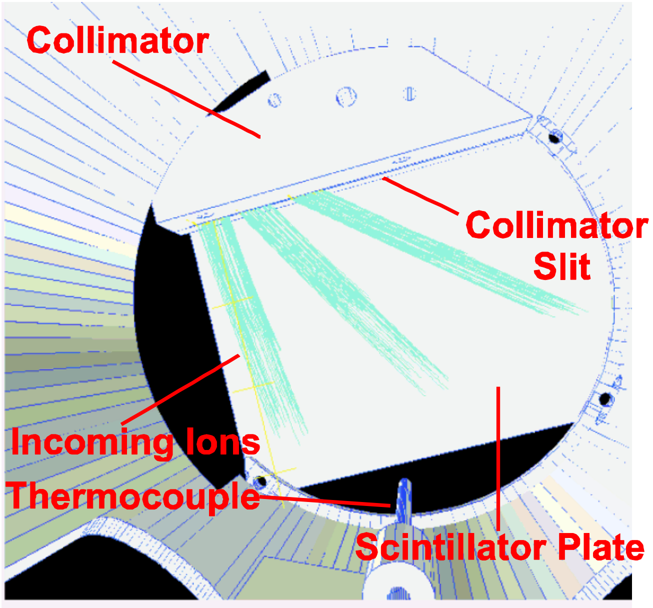

- Secondary plate isolated from the main plate to substrate background noise

FILD Embedded Faraday Cup Measurement Successfully Tested in AUG

Faraday cup measurement embedded in scintillator plate gives time-resolved measurement of absolute flux of impinging ions

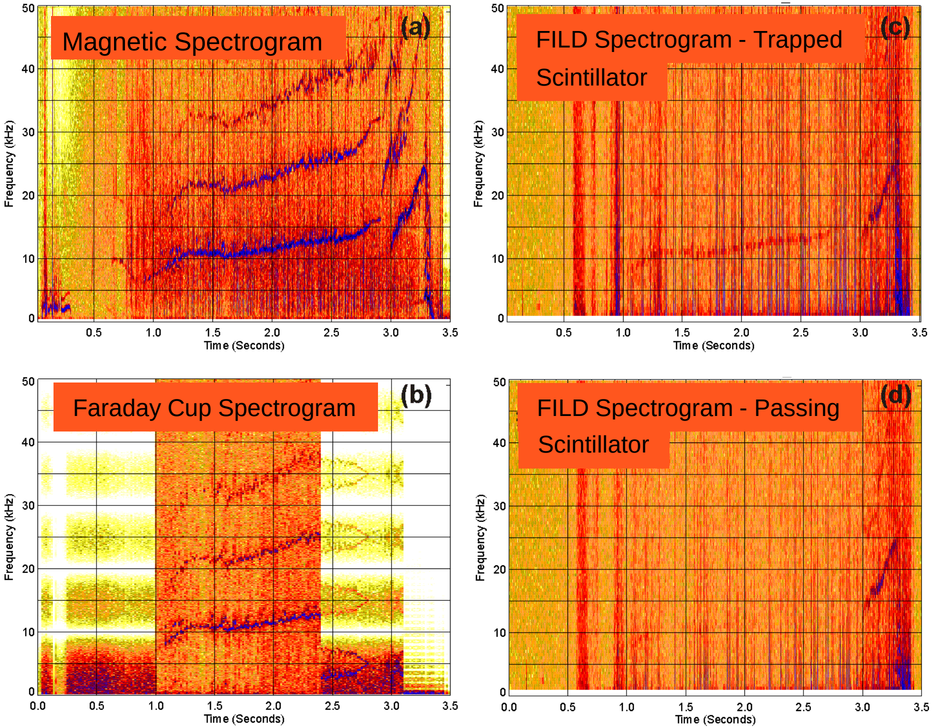

MHD Induced Fast-Ion Losses Can Damage Vacuum Vessel Components

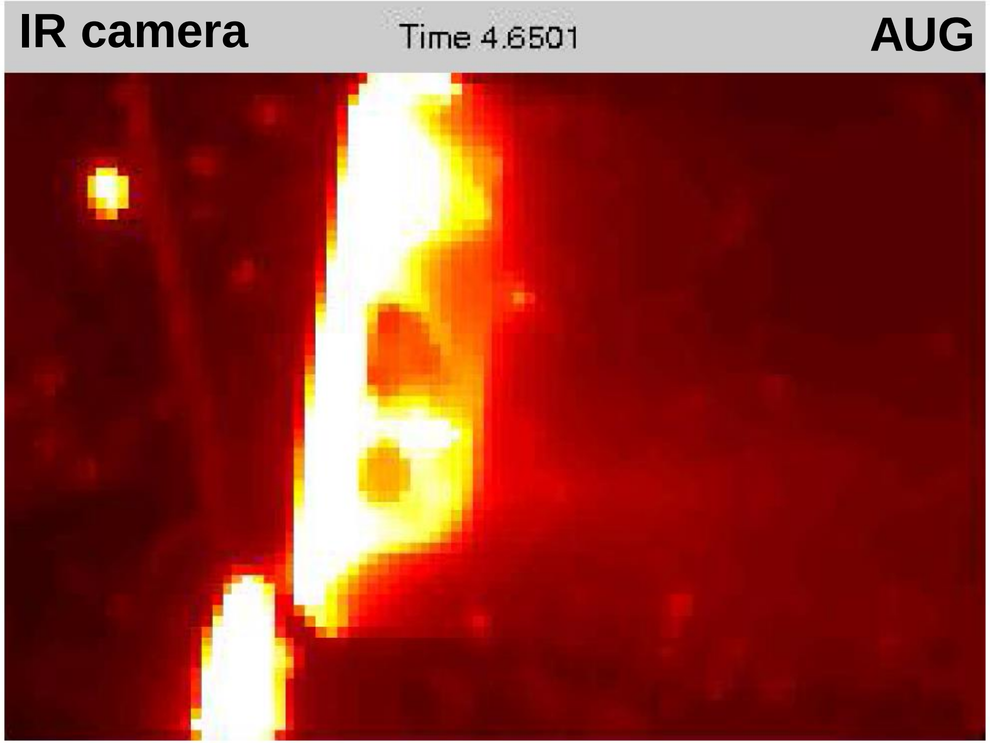

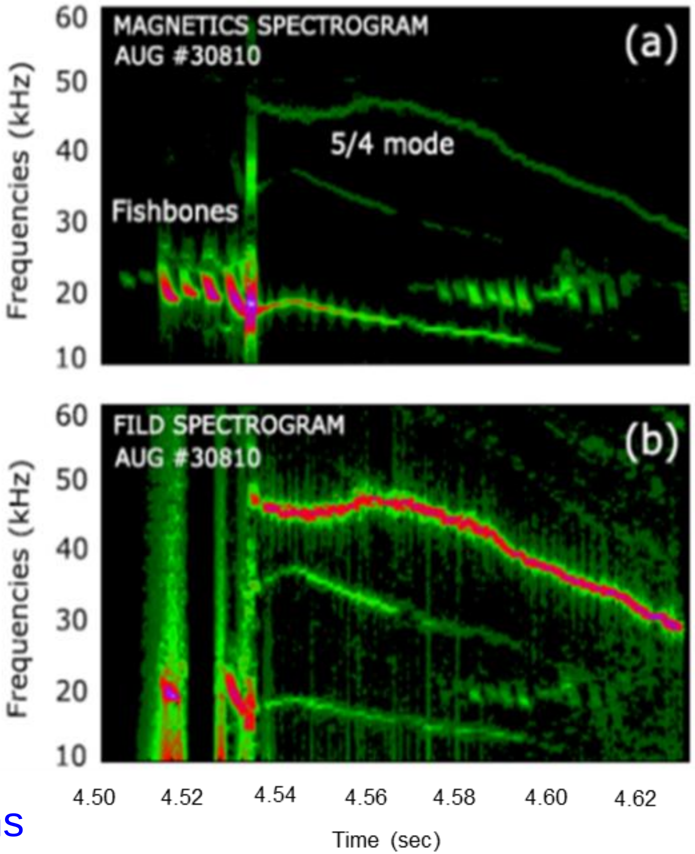

MHz temporal resolution is key to identify MHD fluctuations

MHD Induced Fast-Ion Losses Can Damage Vacuum Vessel Components

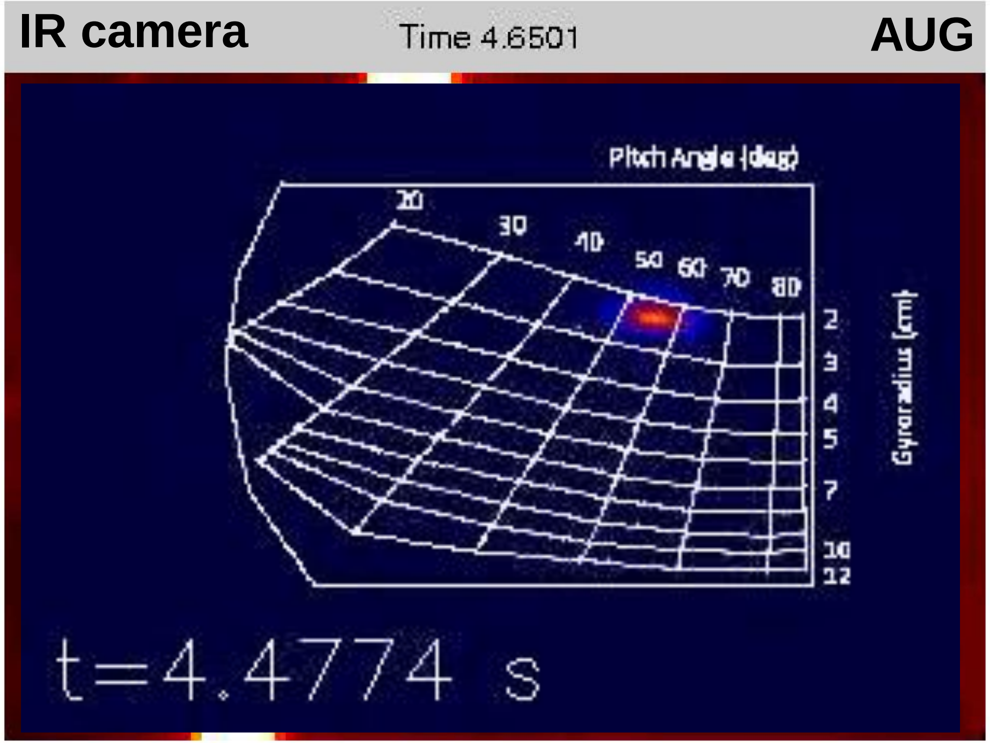

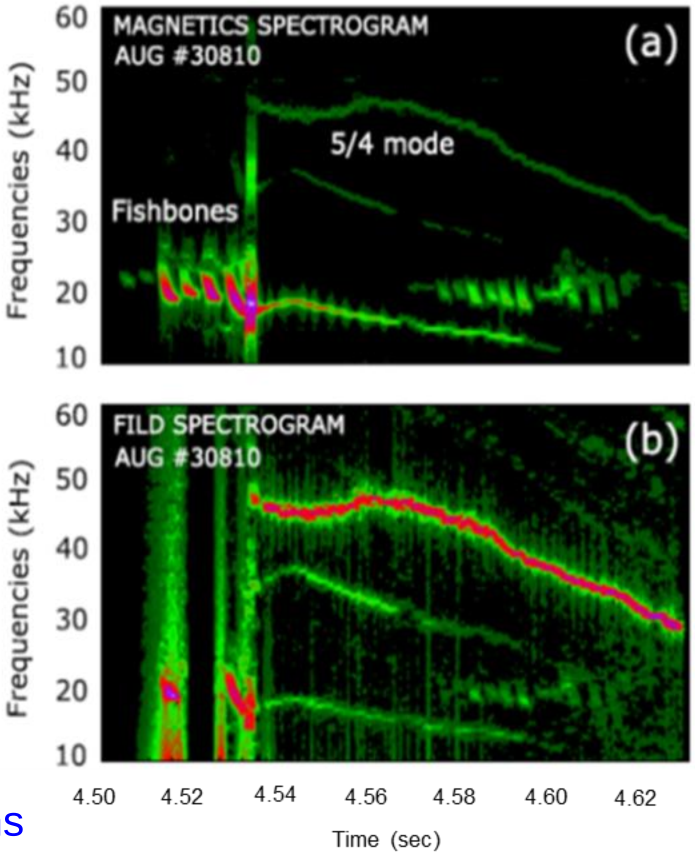

MHz temporal resolution is key to identify MHD fluctuations

Outline

- Requirements of a Fast-Ion Loss Detector
- Scintillator-based Fast-Ion Loss Detector (FILD)
- **Fast-Ion Losses Induced by:**
  - **Alfven Eigenmodes**
  - **Externally Applied Resonant Magnetic Perturbations**
  - **Edge Localized Modes (ELMs)**
- Radial Profiles of Fast-Ion Losses
- Synthetic FILD (FILDSIM)

Alfvenic Temporal Resolution is Key to Identify Loss Mechanisms

M. Garcia-Munoz *et al.*, PRL 2010

- Coherent and incoherent components of FILD signal identify convective and diffusive losses

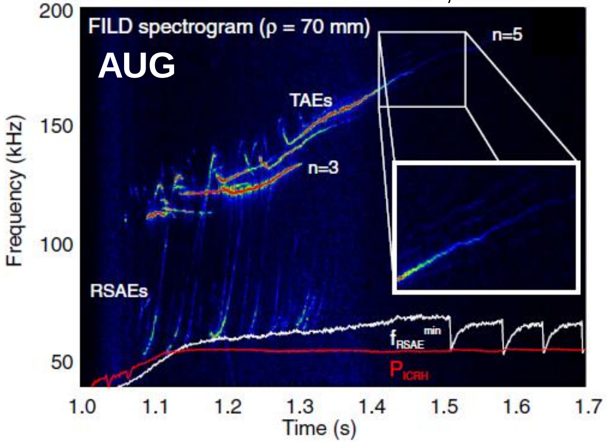

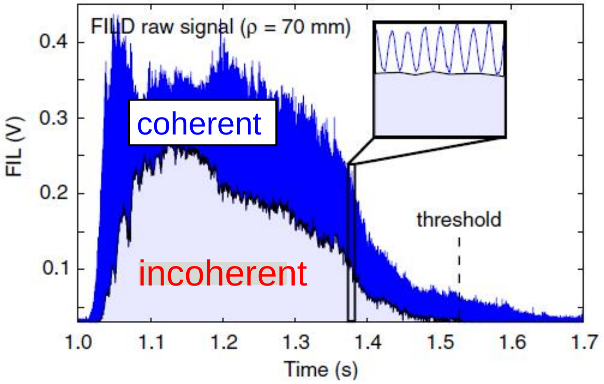

Alfvenic Temporal Resolution is Key to Identify Loss Mechanisms

- Coherent and incoherent components of FILD signal identify convective and diffusive losses
- Coherent losses have **linear** dependence with perturbation amplitude indicating **convective** character
- Incoherent losses have **quadratic** dependence on perturbation amplitude indicating **diffusive** character

M. Garcia-Munoz *et al.*, PRL 2010

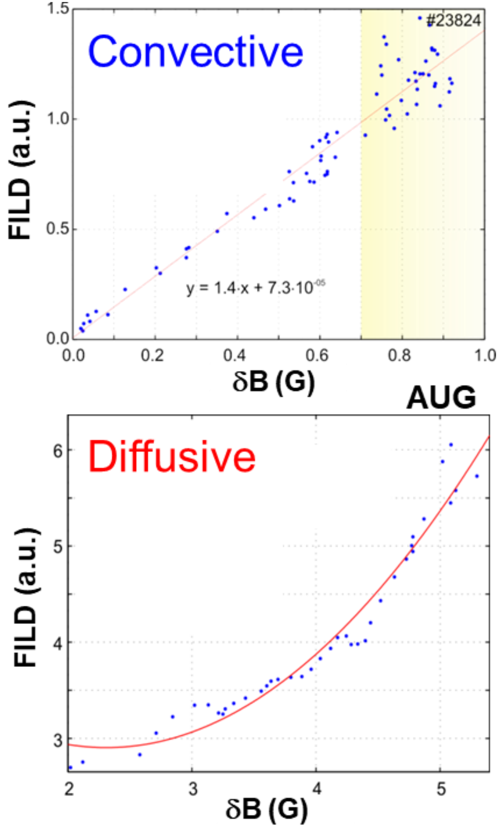

Static n=2 MPs Cause Strong Fast-Ion Losses at Low q_{95} and Density / Collisionality

As density / collisionality increases, fast-ion losses become weaker

- **Fast-ion losses and density pump-out follow same collisionality trend**

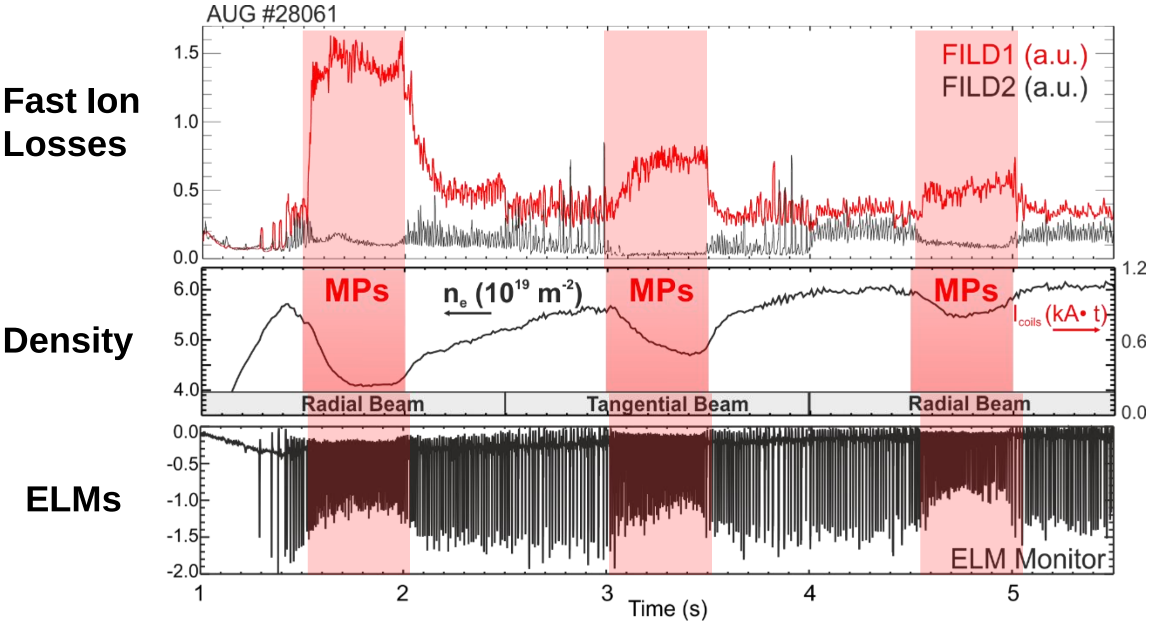

FILD1/FILD2 signals show clear toroidal asymmetry in fast-ion losses

M. Garcia-Munoz et al., Plasma Phys. Control. Fusion **55,** 124014 (2013)

FILD Measures Significant Changes in Escaping Ion Velocity-Space with MPs

- Without MPs, only velocity-space areas corresponding to prompt losses are observed

- During MP phase, multiple additional pitch-angles and energies are observed

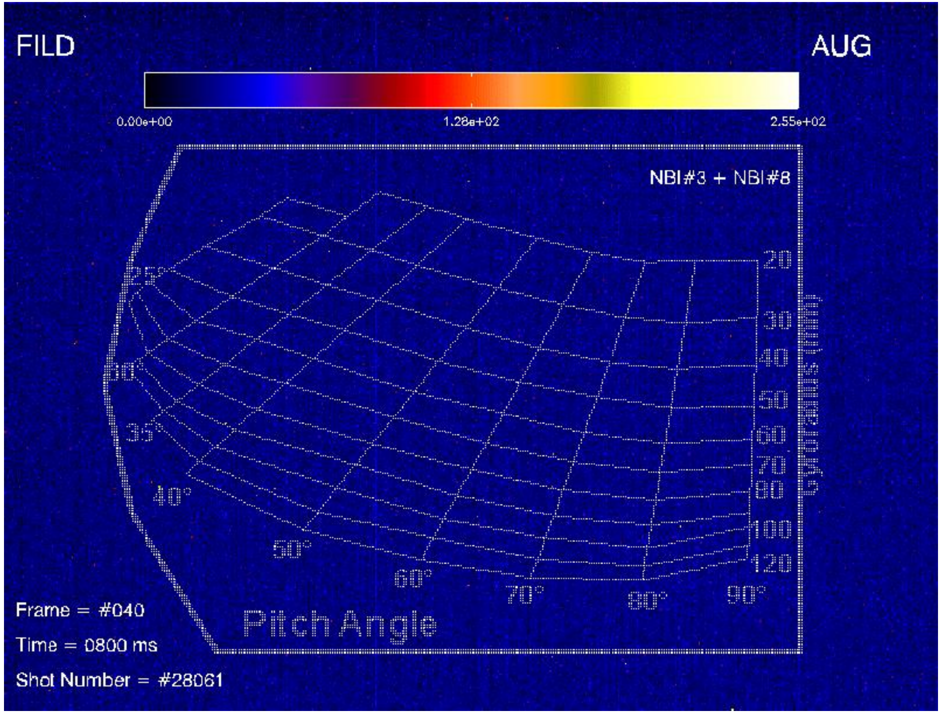

M. Garcia-Munoz et al., Plasma Phys. Control. Fusion **55,** 124014 (2013)

FILD Measures Significant Changes in Escaping Ion Velocity-Space with MPs

- Without MPs, only velocity-space areas corresponding to prompt losses are observed
- During MP phase, multiple additional pitch-angles and energies are observed

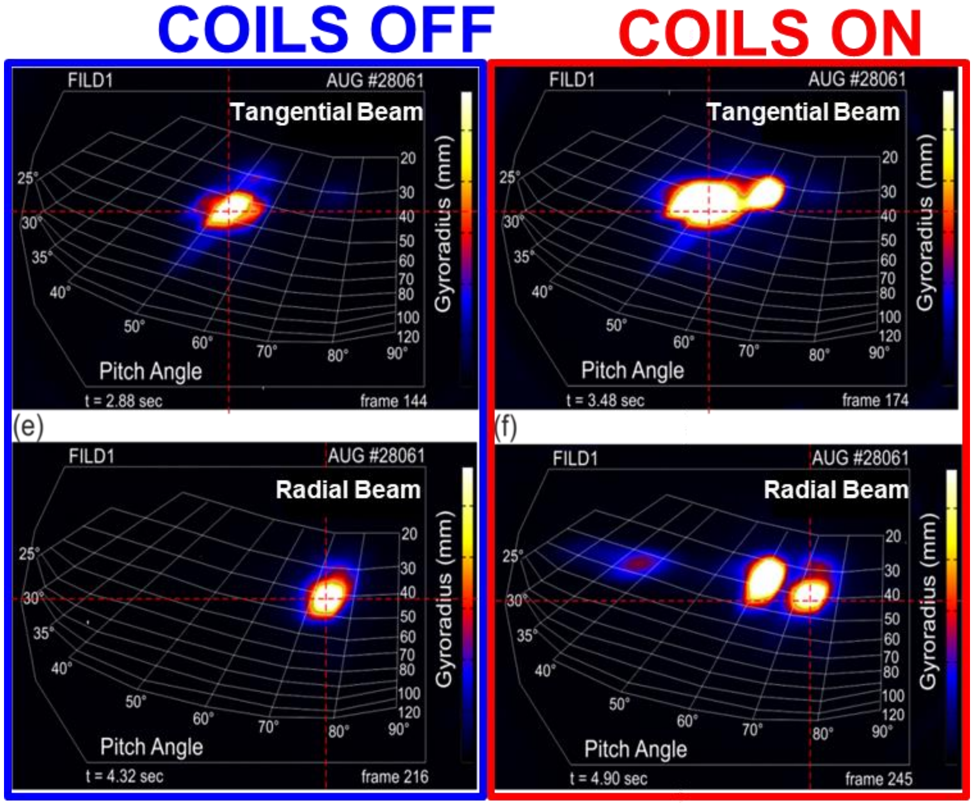

M. Garcia-Munoz et al., Plasma Phys. Control. Fusion **55,** 124014 (2013)

Measured fast-ion losses due to MPs can be up to an order of magnitude higher than nominal NBI prompt losses w/o MPs

During MP phase bursting ELM induced fast-ion losses are replaced by DC losses

Without MPs, fast-ion losses are:

- NBI prompt losses (DC component)
- Bursting ELM induced fast-ion losses

Different fast-ion temporal response to increasing (10 ms) and decaying (200 ms) MP

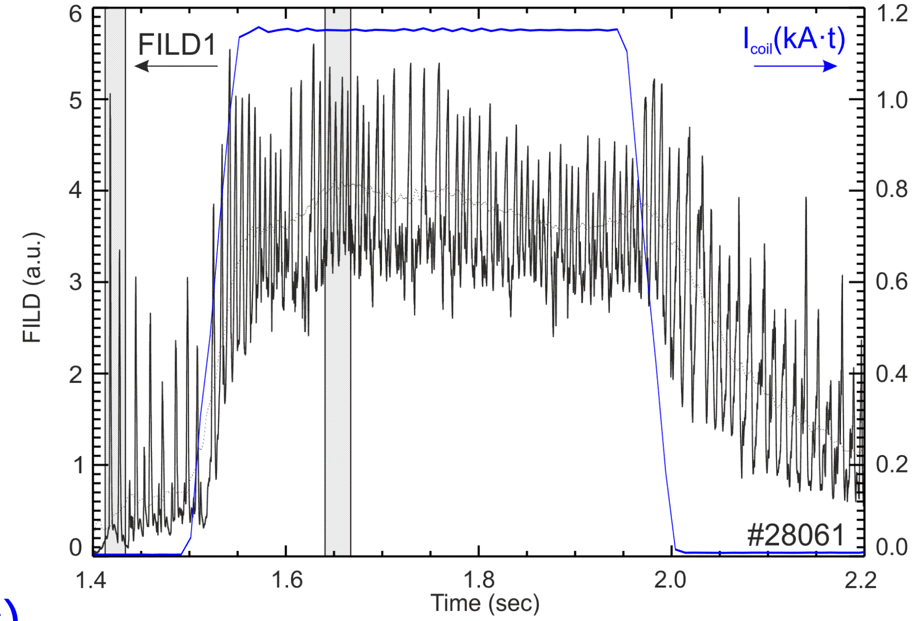

ELM Induced Fast-Ion Losses Are Routinely Observed in H-Mode Discharges

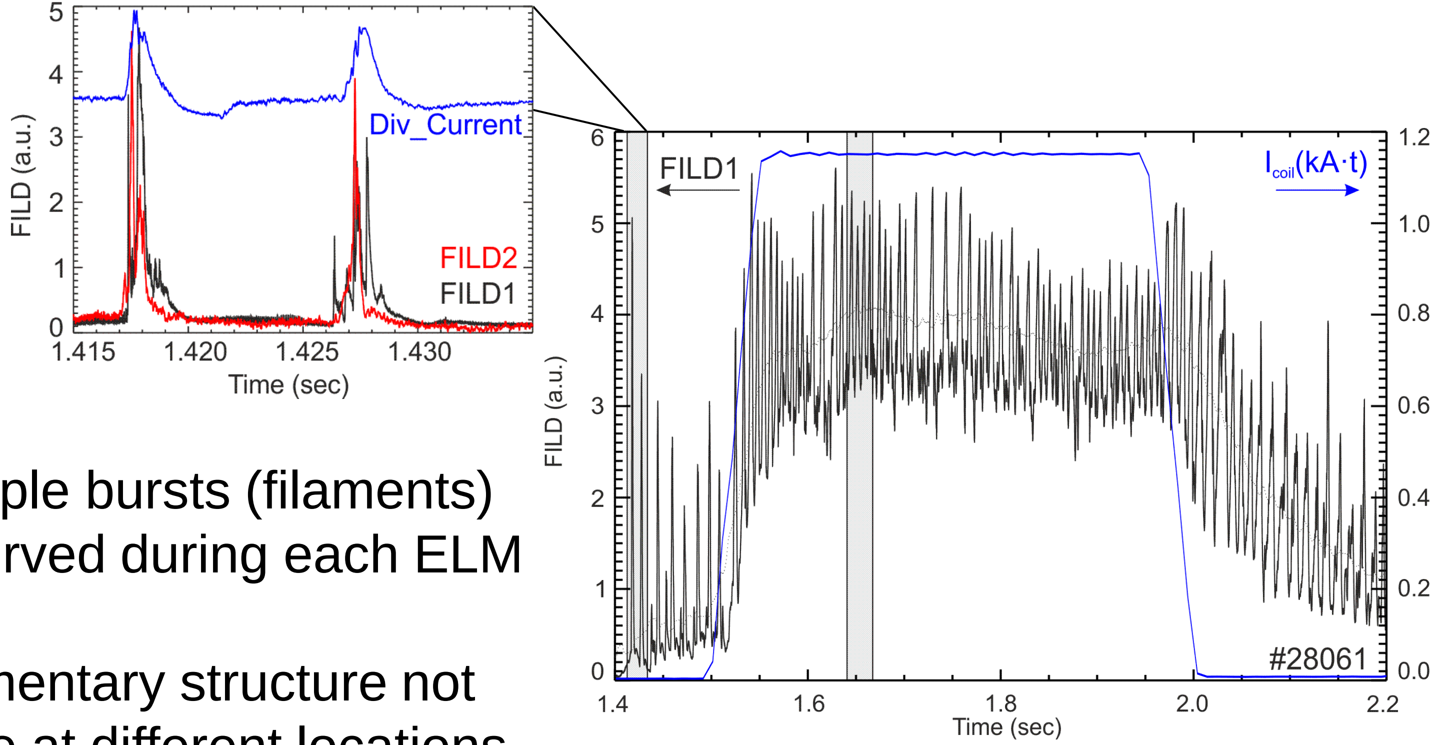

- Multiple bursts (filaments) observed during each ELM

- Filamentary structure not same at different locations (FILD1 vs FILD2)

ELM Induced Fast-Ion Losses Are Routinely Observed in H-Mode Discharges

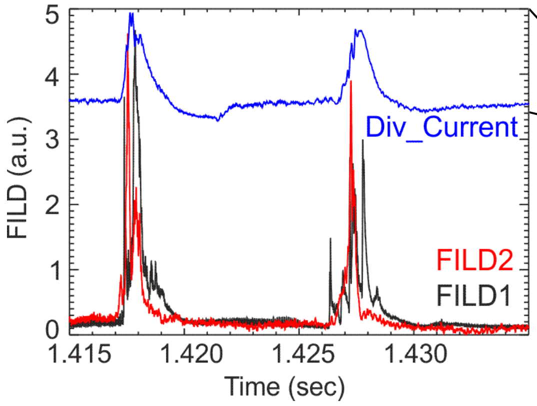

Efficient resonant transport mechanism

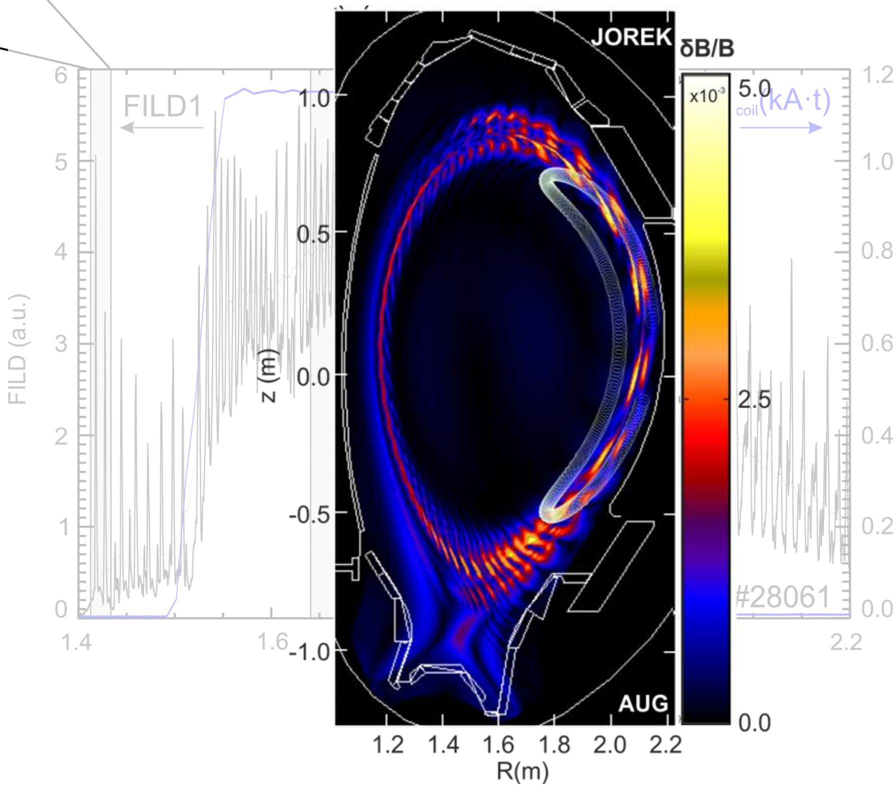

- ➢ Multiple bursts (filaments) observed during each ELM
- ➢ Filamentary structure not same at different locations (FILD1 vs FILD2)

Outline

- Requirements of a Fast-Ion Loss Detector
- Scintillator-based Fast-Ion Loss Detector (FILD)
- Fast-Ion Losses Induced by:
  - Alfven Eigenmodes
  - Externally Applied Resonant Magnetic Perturbations
  - Edge Localized Modes (ELMs)
- **Radial Profiles of Fast-Ion Losses**
- Synthetic FILD (FILDSIM)

FILD Radial Profiles To Covers a Volume in Phase-Space

- Phase-space coordinates (E, μ, P_{φ}) are constant along fast-ion trajectory

- FILD covers a 2D surface in phase-space of the fast-ion distribution edge

E: Particle energy

μ: Magnetic moment

P_{φ}: Toroidal canonical momentum

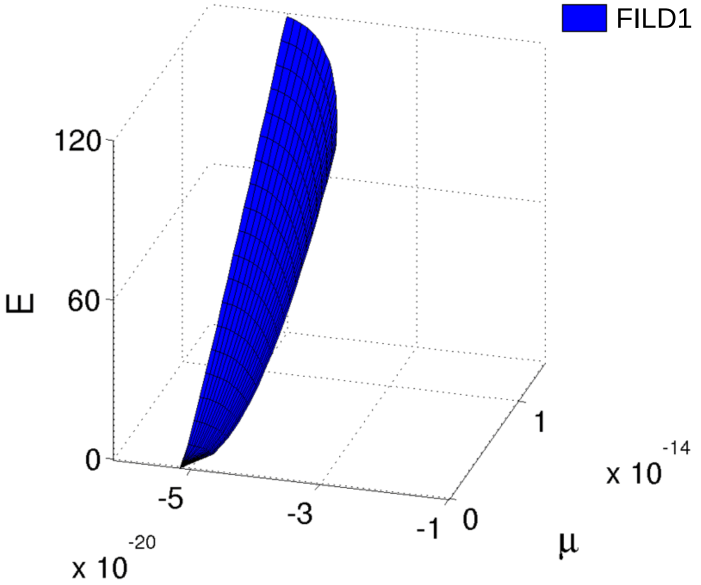

J. Gonzalez-Martin et al., HTPD 2020

FILD Radial Profiles To Covers a Volume in Phase-Space

- Phase-space coordinates (E, μ, P_φ) are constant along fast-ion trajectory

- FILD covers a 2D surface in phase-space of the fast-ion distribution edge

E: Particle energy

μ: Magnetic moment

P_φ: Toroidal canonical momentum

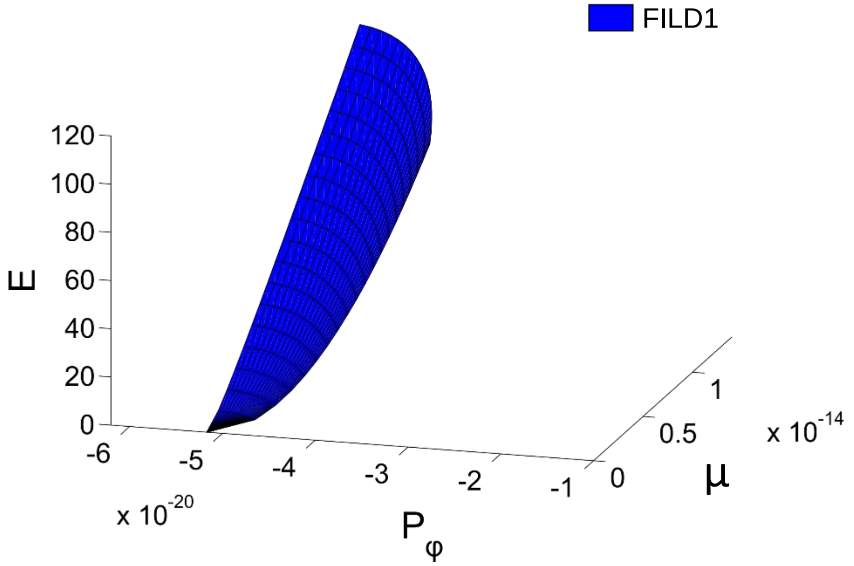

J. Gonzalez-Martin et al., HTPD 2020

FILD Radial Profiles To Covers a Volume in Phase-Space

- Phase-space coordinates (E, μ, P_φ) are constant along fast-ion trajectory

- FILD covers a 2D surface in phase-space of the fast-ion distribution edge

E: Particle energy

μ: Magnetic moment

P_φ: Toroidal canonical momentum

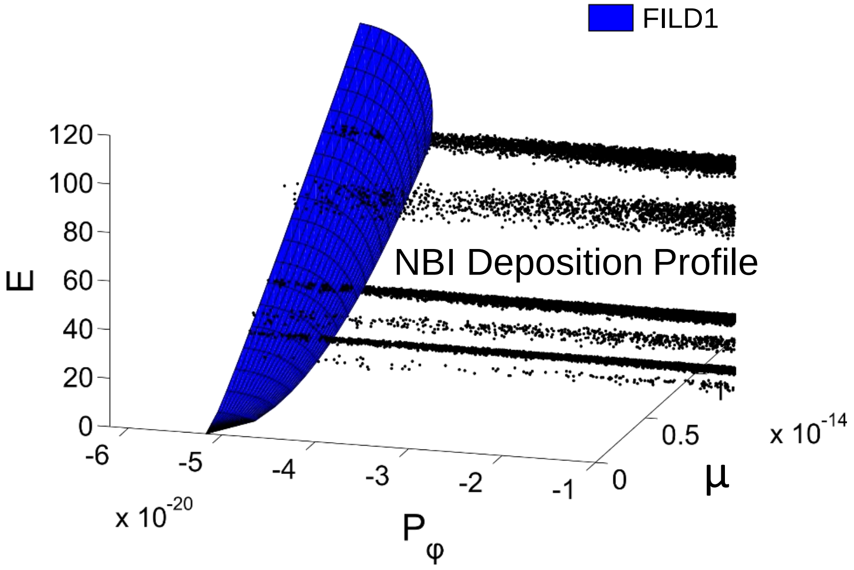

J. Gonzalez-Martin et al., HTPD 2020

FILD Radial Profiles To Covers a Volume in Phase-Space

- Phase-space coordinates (E, μ, P_φ) are constant along fast-ion trajectory

- FILD covers a 2D surface in phase-space of the fast-ion distribution edge

- FILD poloidal array increases phase-space coverage and diagnoses 3D losses
  - ➢ TF ripple, externally applied MPs, MHD…

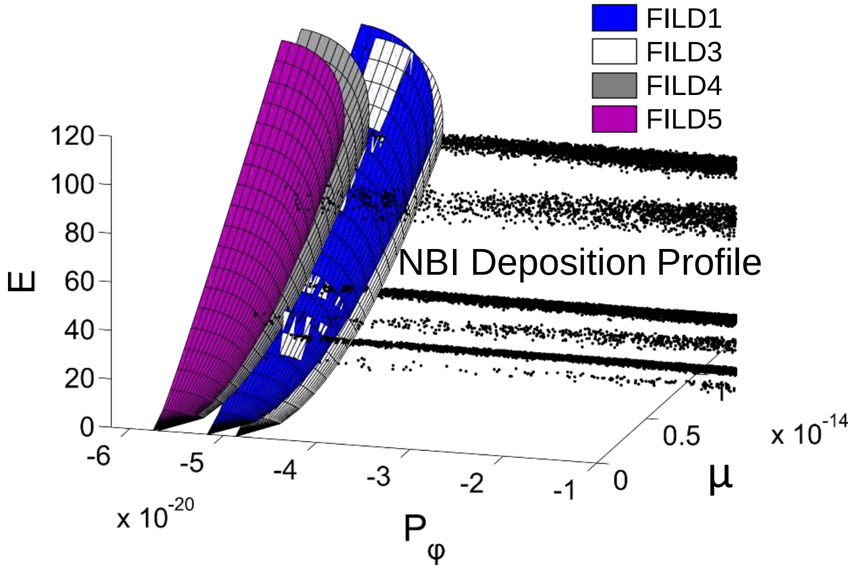

FILD Radial Profiles To Covers a Volume in Phase-Space

- Phase-space coordinates (E, μ, P_φ) are constant along fast-ion trajectory

- FILD covers a 2D surface in phase-space of the fast-ion distribution edge

- FILD poloidal array increases phase-space coverage and diagnoses 3D losses
  - ➢ TF ripple, externally applied MPs, MHD…

- New FILD sweeping enables diagnosing a 3D phase-space volume

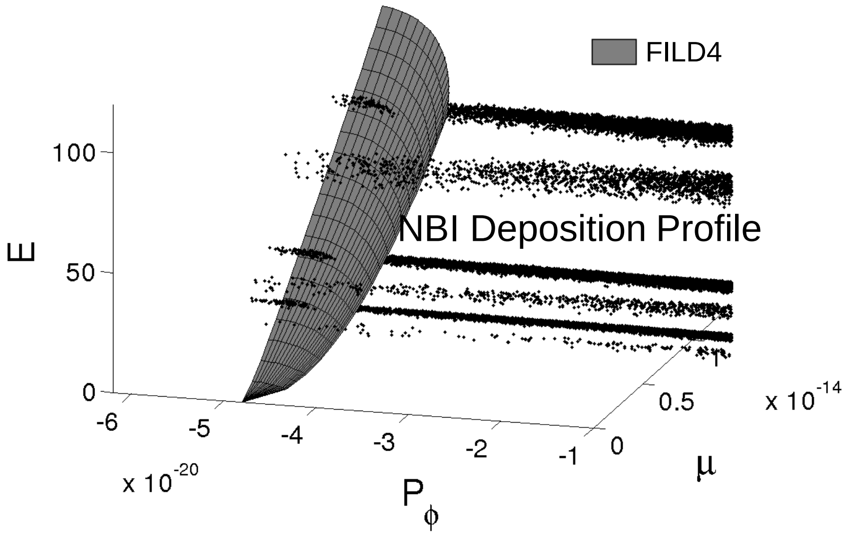

FILD4 Inserted by a Magnetically Driven Manipulator

- In-situ system installed under ECRH mirror holder w/o mechanical contact with a port plug

- Probe head is pulled back by a retaining spring

- Energized coil tries to align with AUG toroidal field producing a torque that overcome retaining spring force*

- Coil energized within 5ms by DCS via a programmable power supply

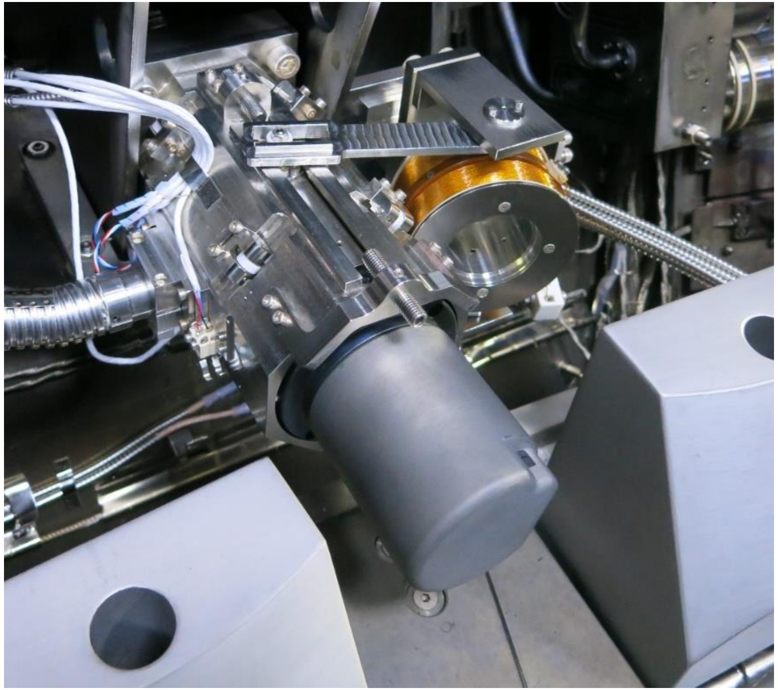

J. Gonzalez-Martin *et al* 2019 JINST 14 C11005

*Similar to A. Schmid, A. Herrmann et *al.*, RSI **78**, 053502 (2007) and J. P Gunn and J.Y. Pascal, RSI **82**, 123505 (2011)

FILD4 Inserted by a Magnetically Driven Manipulator

- In-situ system installed under ECRH mirror holder w/o mechanical contact with a port plug
- Probe head is pulled back by a retaining spring
- Energized coil tries to align with AUG toroidal field producing a torque that overcome retaining spring force*
- Coil energized within 5ms by DCS via a programmable power supply

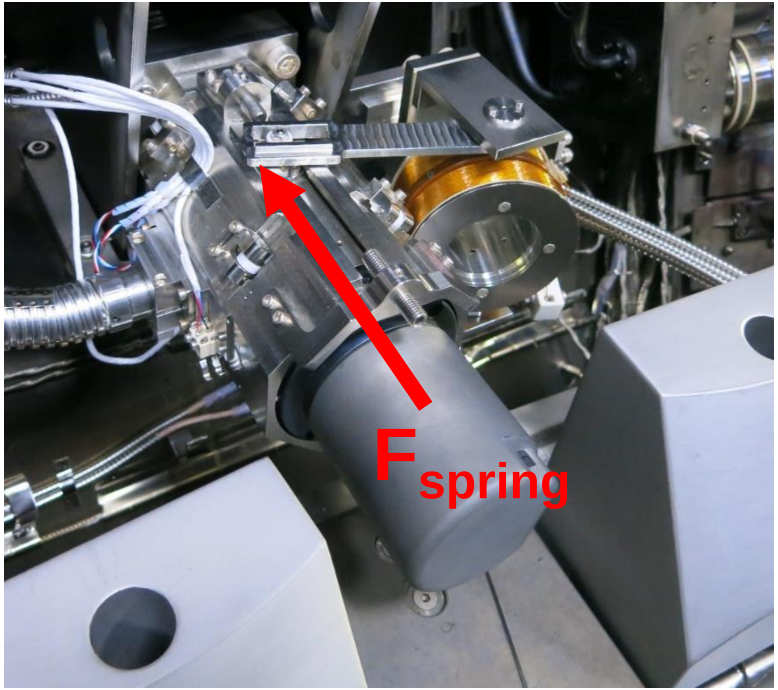

J. Gonzalez-Martin *et al* 2019 JINST 14 C11005

*Similar to A. Schmid, A. Herrmann et *al.*, RSI **78**, 053502 (2007) and J. P Gunn and J.Y. Pascal, RSI **82**, 123505 (2011)

FILD4 Inserted by a Magnetically Driven Manipulator

- In-situ system installed under ECRH mirror holder w/o mechanical contact with a port plug
- Probe head is pulled back by a retaining spring
- Energized coil tries to align with AUG toroidal field producing a torque that overcome retaining spring force*
- Coil energized within 5ms by DCS via a programmable power supply

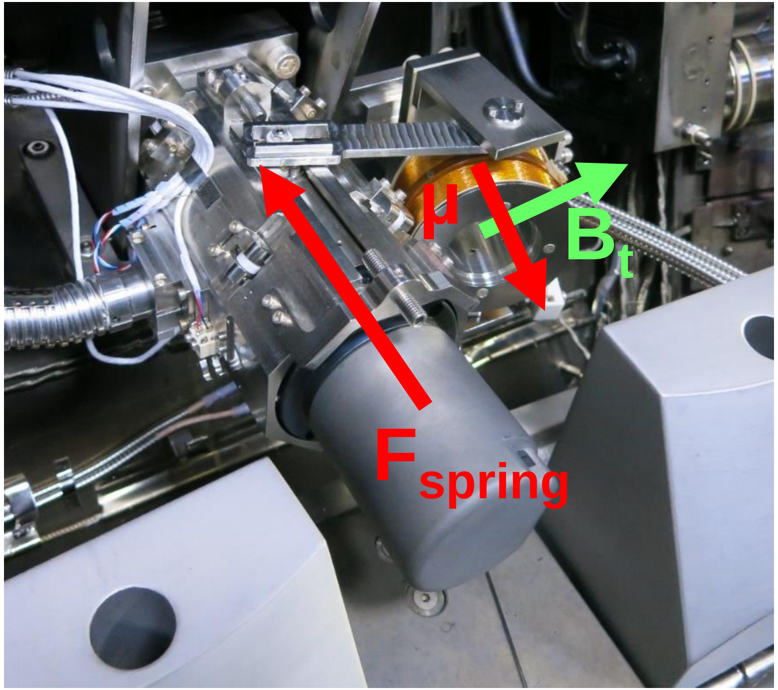

J. Gonzalez-Martin *et al* 2019 JINST 14 C11005

*Similar to A. Schmid, A. Herrmann et *al.*, RSI **78**, 053502 (2007) and J. P Gunn and J.Y. Pascal, RSI **82**, 123505 (2011)

FILD4 Inserted by a Magnetically Driven Manipulator

- In-situ system installed under ECRH mirror holder w/o mechanical contact with a port plug
- Probe head is pulled back by a retaining spring
- Energized coil tries to align with AUG toroidal field producing a torque that overcome retaining spring force*
- Coil energized within 5ms by DCS via a programmable power supply

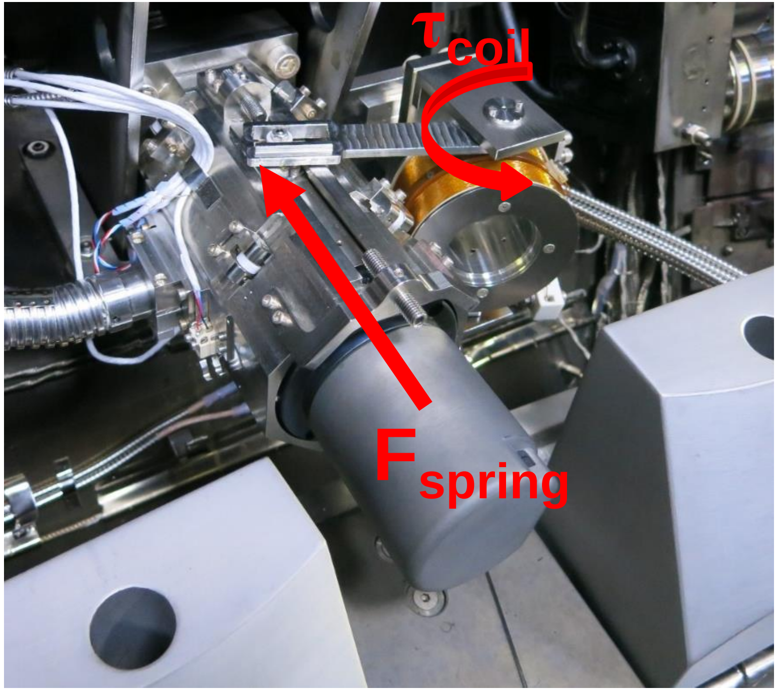

J. Gonzalez-Martin *et al* 2019 JINST 14 C11005

*Similar to A. Schmid, A. Herrmann et *al.*, RSI **78**, 053502 (2007) and J. P Gunn and J.Y. Pascal, RSI **82**, 123505 (2011)

FILD Swept to Obtain Radial Measurements

- 25mm profiles of fast-ion losses every ~200ms
- FILD detects both NBI and ICRH fast-ions

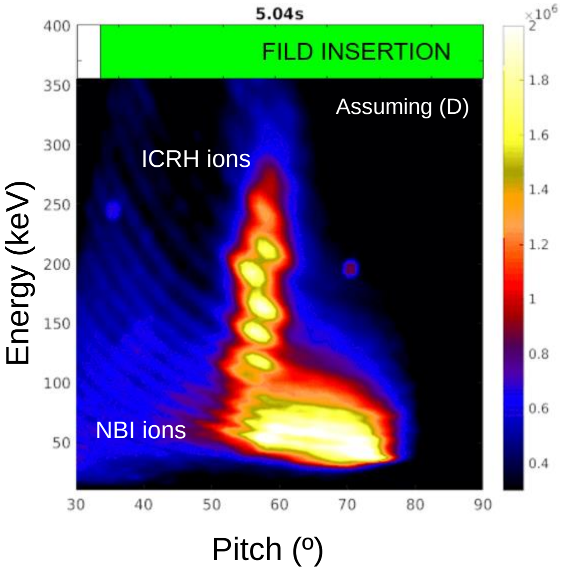

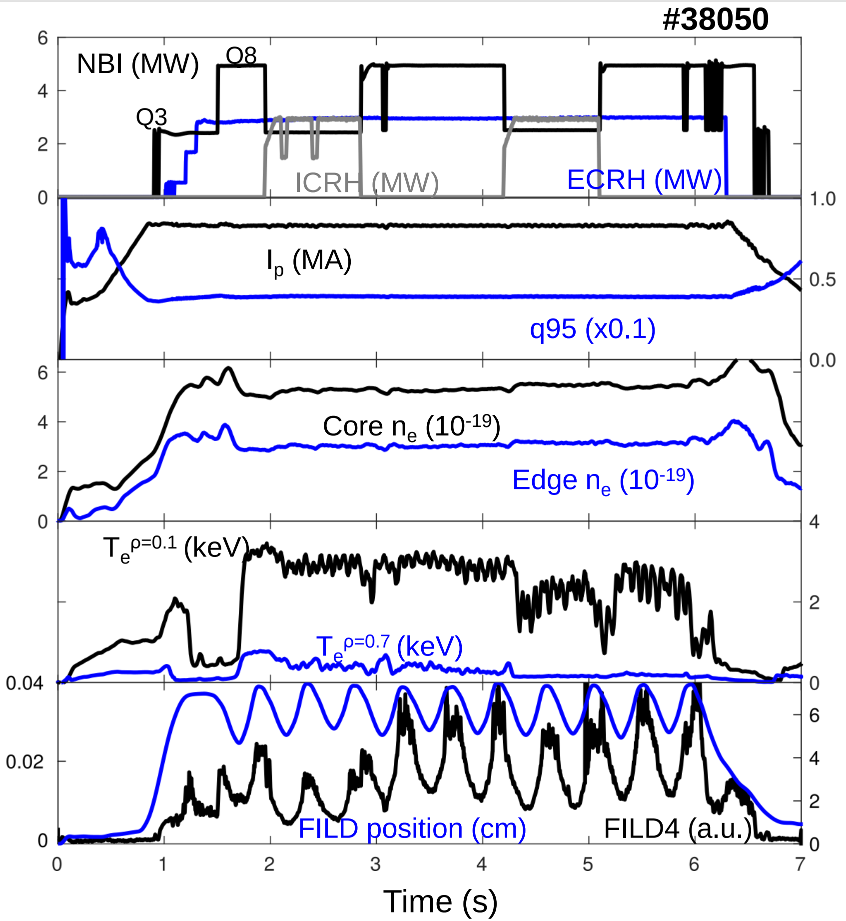

FILD Swept to Obtain Radial Measurements

- 25mm profiles of fast-ion losses every ~200ms
- FILD detects both NBI and ICRH fast-ions

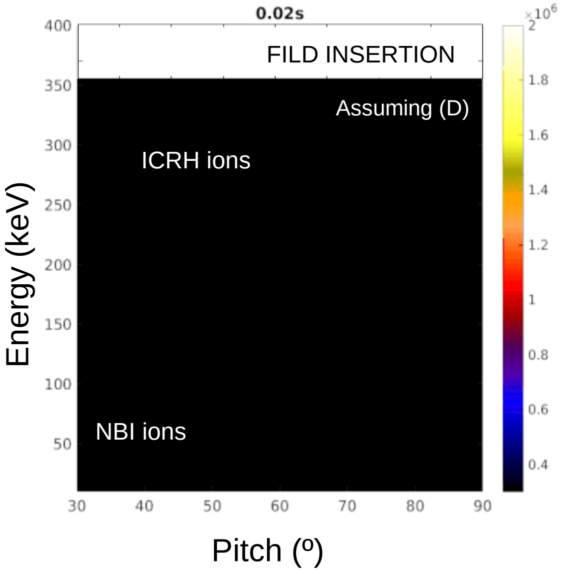

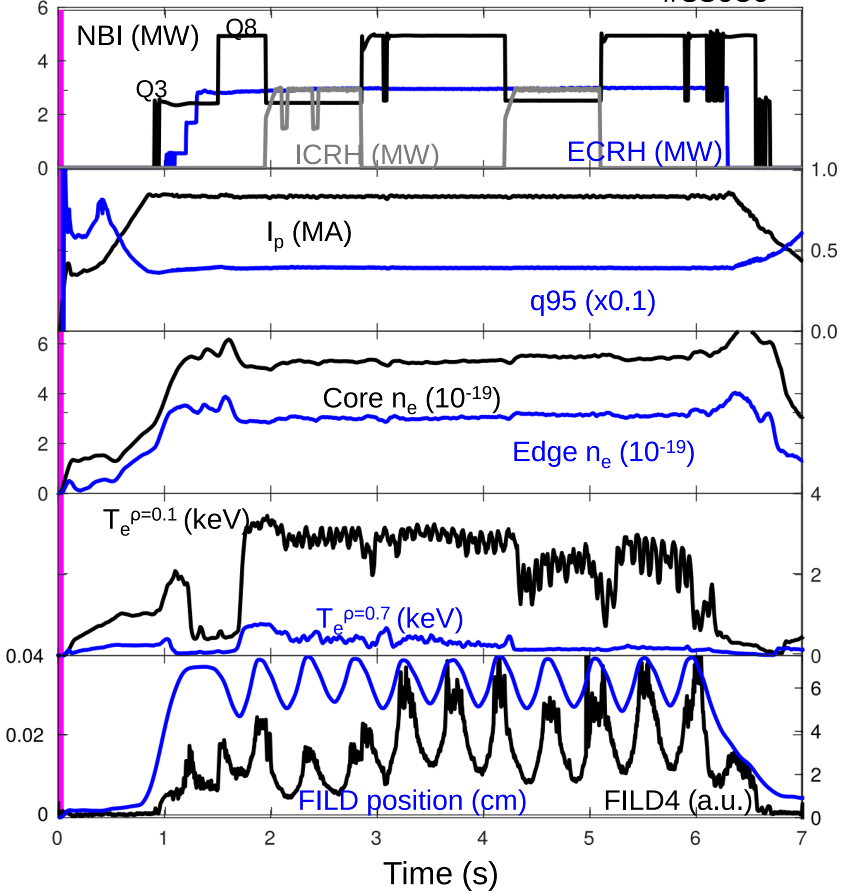

Radially-Resolved Velocity-Space Measurements

- Radial measurements are a combination of:

  - Time-resolved velocity-space measurements
  - Time-resolved FILD location

FILD = FILD(E,Pitch,t)

+

$R_{FILD} = R_{FILD}(t)$

↓

FILD = FILD(E,Pitch,R_{FILD})

Radially-Resolved Velocity-Space Measurements

- Radial measurements are a combination of:

  - Time-resolved velocity-space measurements
  - Time-resolved FILD location

FILD(E,Pitch,R_{FILD})

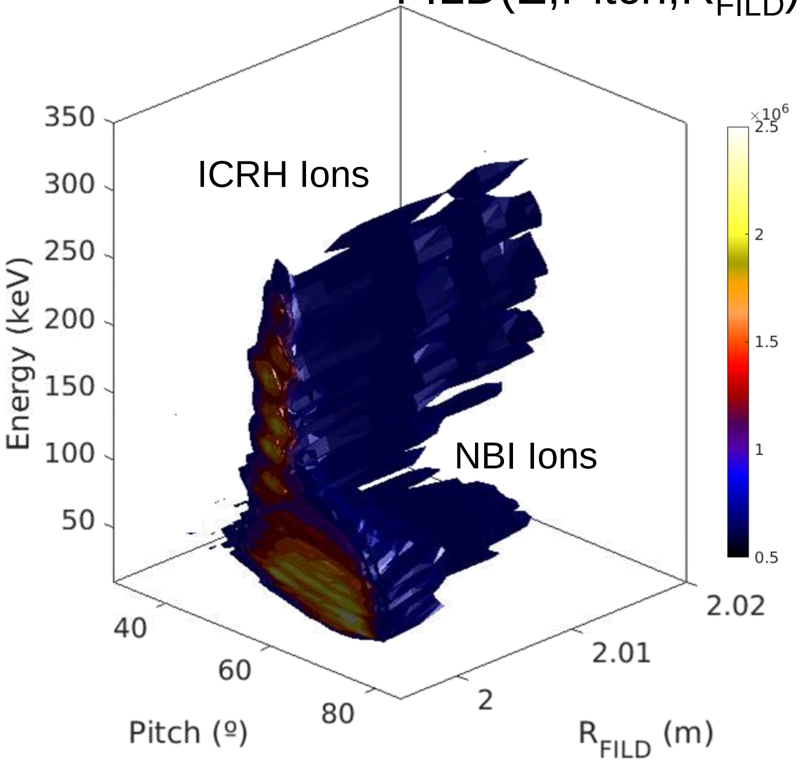

NBI and ICRH Ions Show Different Radial Dependence

- Regions of interest are defined on velocity-space and plotted radially

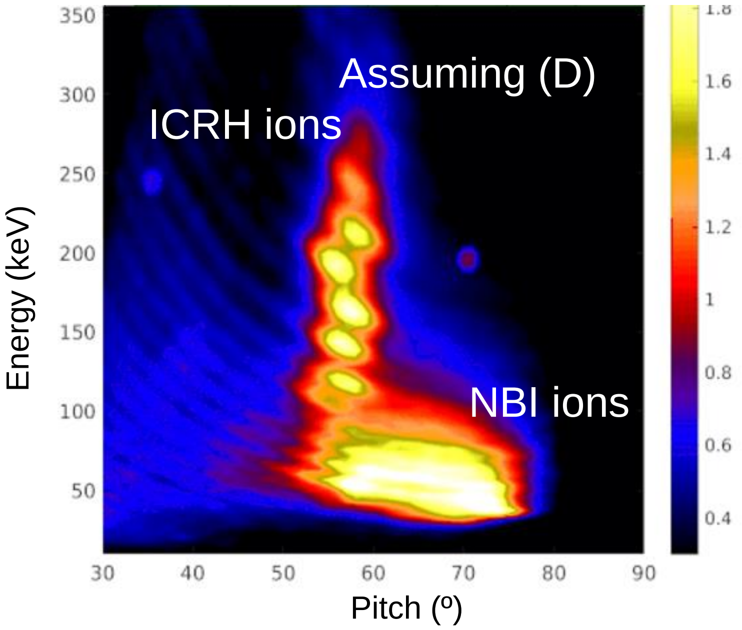

NBI and ICRH Ions Show Different Radial Dependence

- Regions of interest are defined on velocity-space and plotted radially

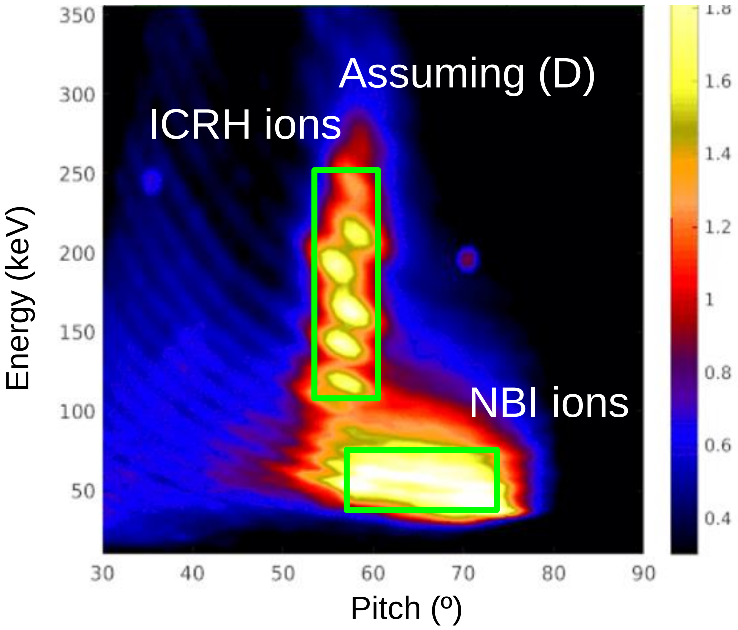

NBI and ICRH Ions Show Different Radial Dependence

- Regions of interest are defined on velocity-space and plotted radially
- NBI ions have larger radial gradient than ICRH ions

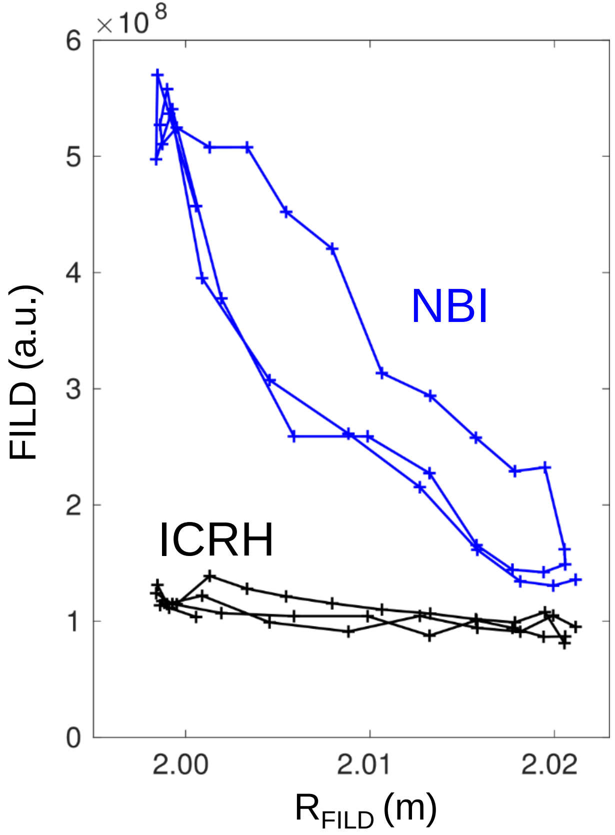

NBI and ICRH Ions Show Different Radial Dependence

- Regions of interest are defined on velocity-space and plotted radially

- NBI ions have larger radial gradient than ICRH ions

- For ICRH ions, each energy has a different radial profile

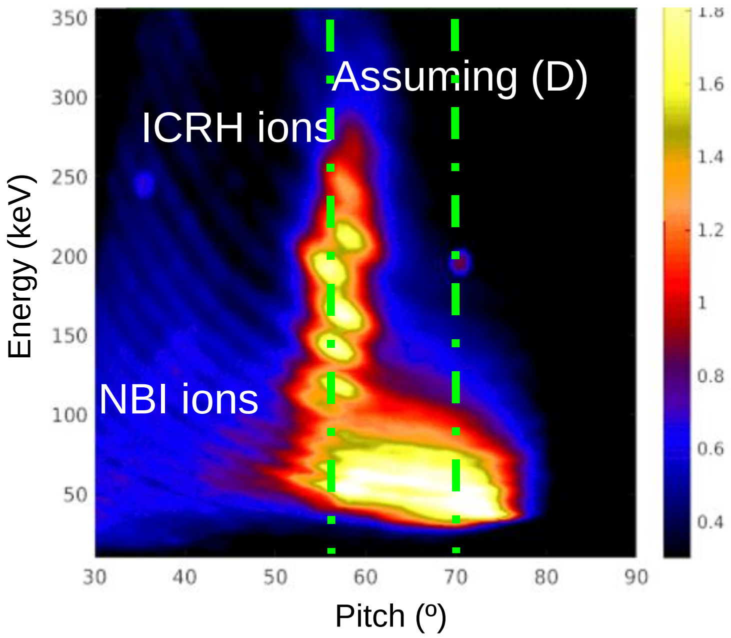

NBI and ICRH Ions Show Different Radial Dependence

- Regions of interest are defined on velocity-space and plotted radially

- NBI ions have larger radial gradient than ICRH ions

- For ICRH ions, each energy has a different radial profile

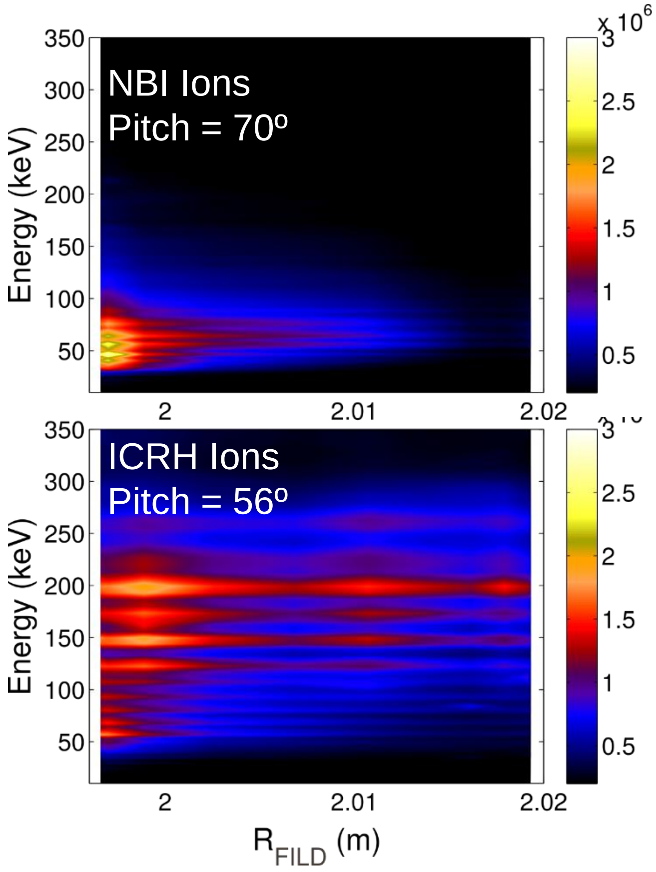

Radial Profile of NBI Losses Depends on Born Location

- Two different pitch angle at injection energy are reproduced by ASCOT*

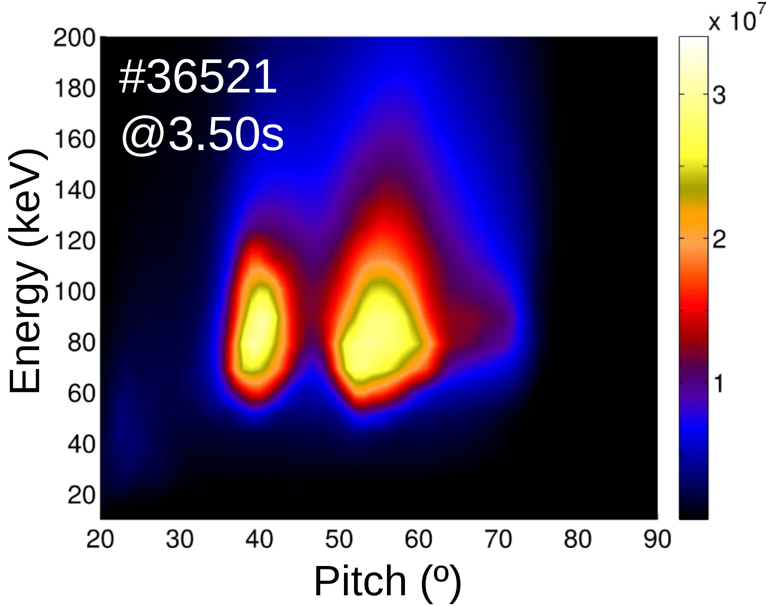

Radial Profile of NBI Losses Depends on Born Location

- Two different pitch angle at injection energy are reproduced by ASCOT*
  - #6 Low field side (Trapped)
  - #8 High field side (Passing)

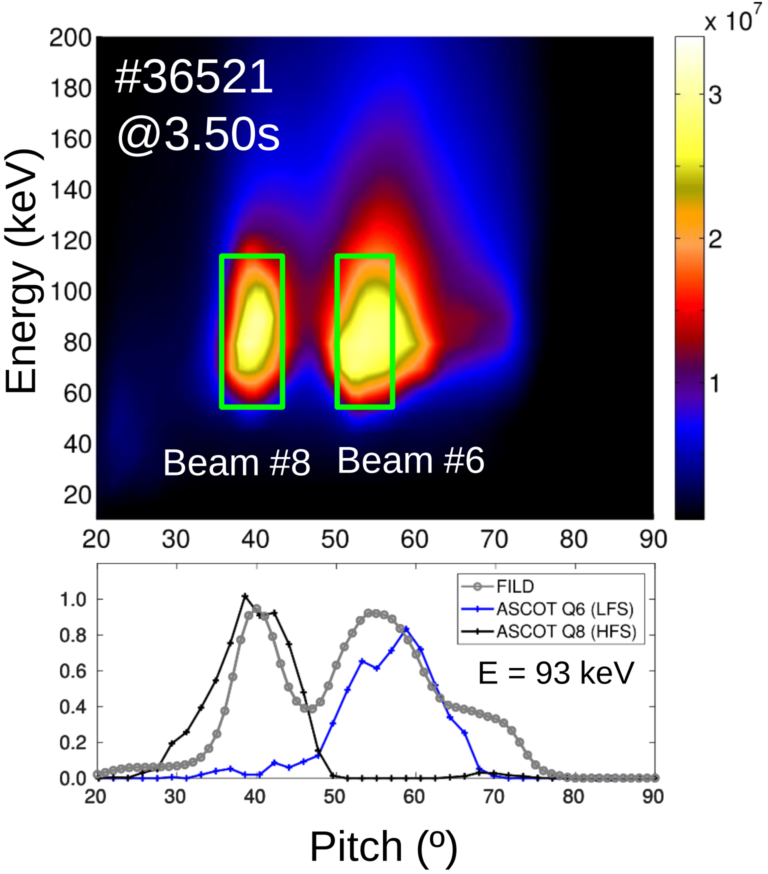

*E. Hirvijoki et al. Computer Phys. Com.**185**, 1310-1321 (2014)

Radial Profile of NBI Losses Depends on Born Location

- Two different pitch angle at injection energy are reproduced by ASCOT*
  - ➢ #6 Low field side (Trapped)
  - ➢ #8 High field side (Passing)

- Particles ionized at the low field side are captured ~1cm earlier by FILD
  - ➢ FILD scans through the passing/lost boundary

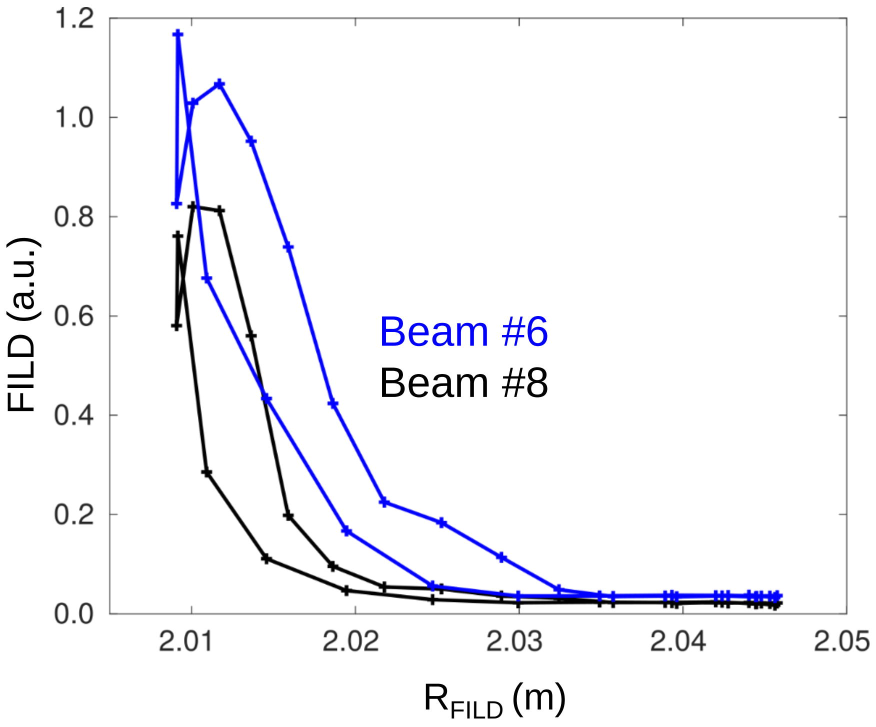

*E. Hirvijoki et al. Computer Phys. Com.**185**, 1310-1321 (2014)

Radial Profile of NBI Losses Depends on Born Location

- Two different pitch angle at injection energy are reproduced by ASCOT*
  - #6 Low field side (Trapped)
  - #8 High field side (Passing)

- Particles ionized at the low field side are captured ~1cm earlier by FILD
  - FILD scans through the passing/lost boundary

- ASCOT reproduces radially-resolved beam deposition profile measurements

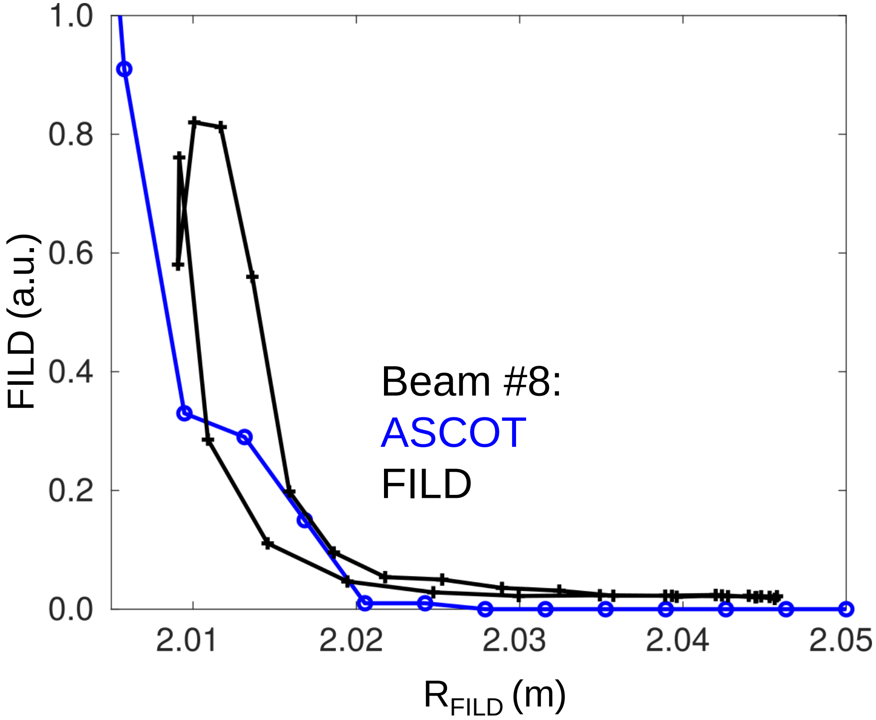

*E. Hirvijoki et al. Computer Phys. Com.**185**, 1310-1321 (2014)

First Radial Measurements of MHD-Induced Fast-Ion Losses

- MHD-induced FIL only observed when FILD is inserted

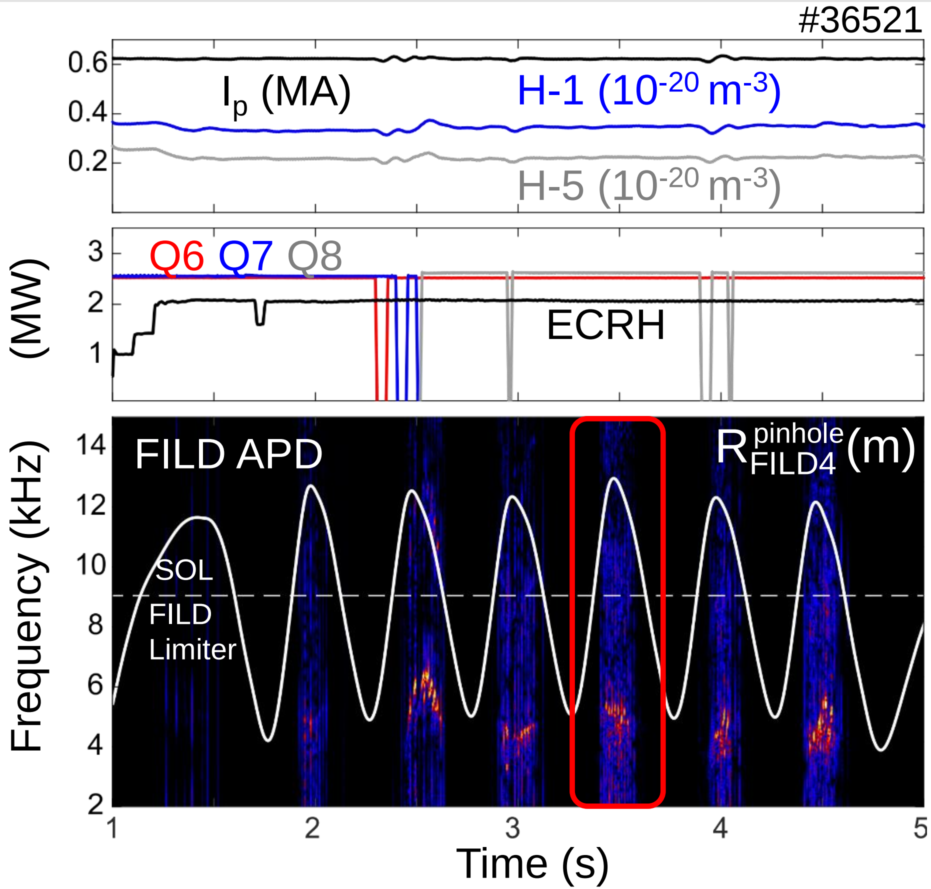

First Radial Measurements of MHD-Induced Fast-Ion Losses

- MHD-induced FIL only observed when FILD is inserted

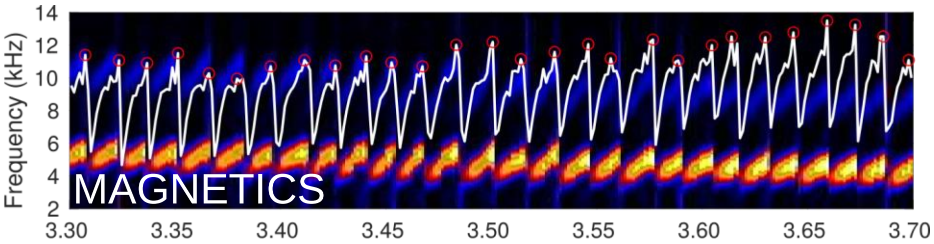

- Around mode local maximum:

First Radial Measurements of MHD-Induced Fast-Ion Losses

- MHD-induced FIL only observed when FILD is inserted

- Around mode local maximum:
    - ➢ Averaged FILD signal (F)

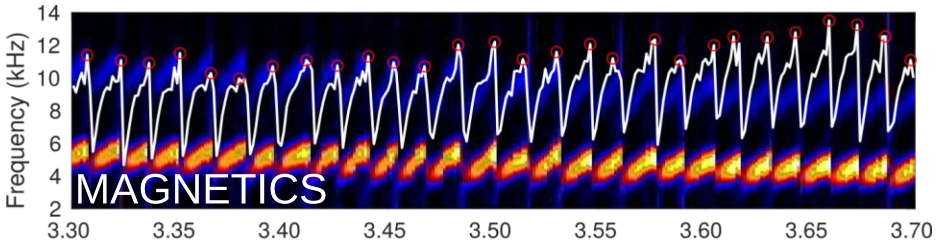

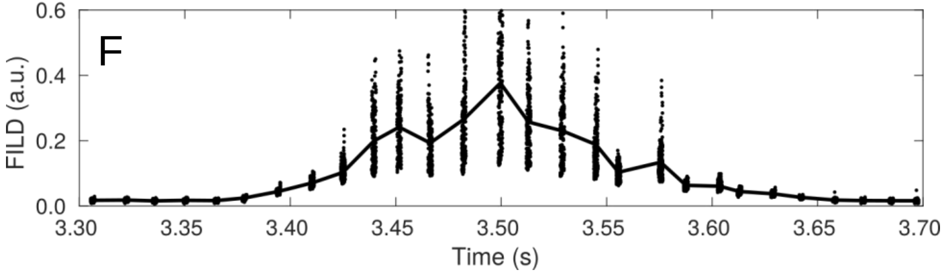

First Radial Measurements of MHD-Induced Fast-Ion Losses

- MHD-induced FIL only observed when FILD is inserted

- Around mode local maximum:
  - ➢ Averaged FILD signal (F)
  - ➢ Convective FILD at mode frequency (ΔF)

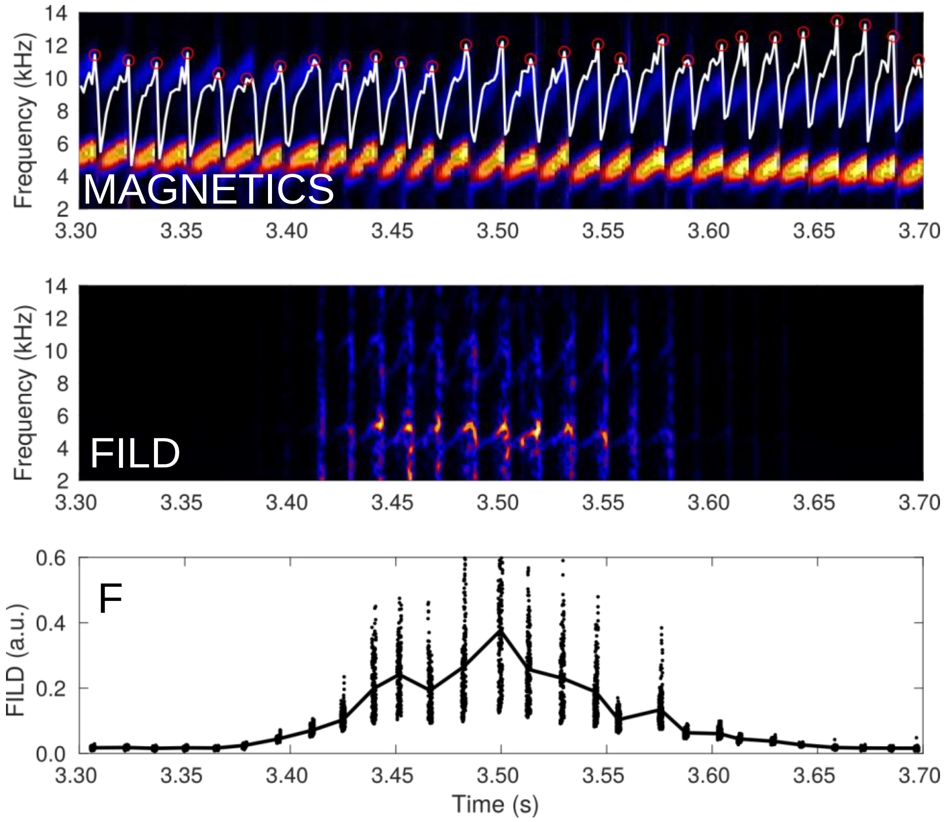

First Radial Measurements of MHD-Induced Fast-Ion Losses

- MHD-induced FIL only observed when FILD is inserted

- Around mode local maximum:
  - ➢ Averaged FILD signal (F)
  - ➢ Convective FILD at mode frequency (ΔF)

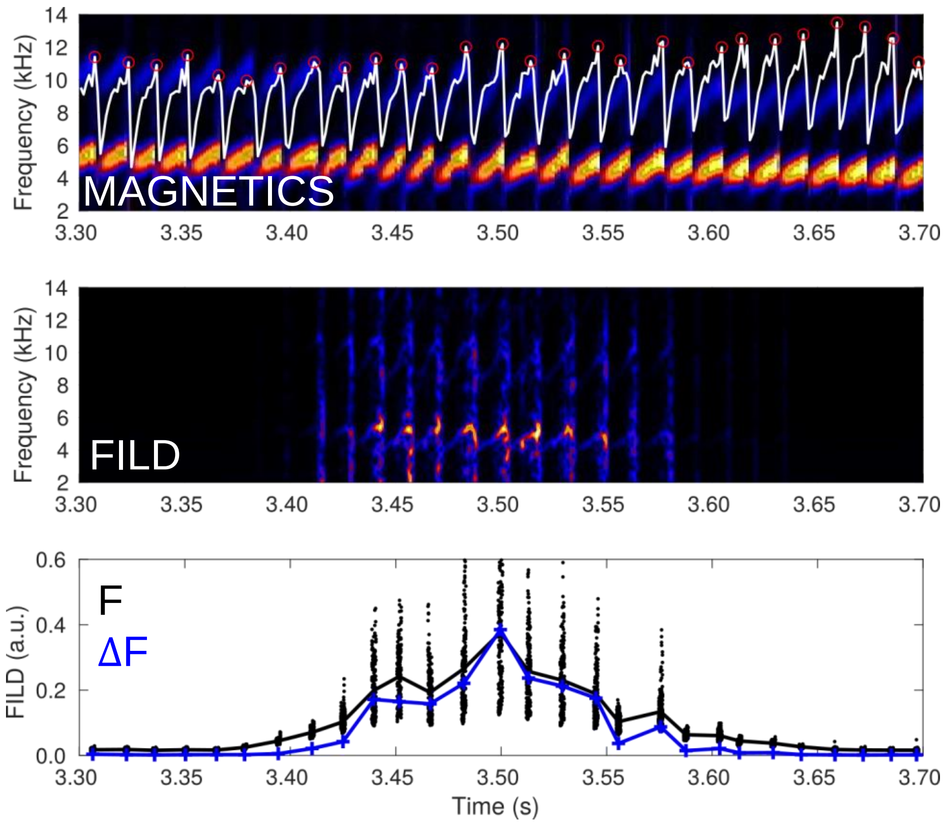

The Light Ion Beam Probe (LIBP) Technique* Uses NBI Prompt Losses to Estimate Orbit Deflection (ξ)

- Provides experimental estimation of fast-ion orbit displacement due to internal perturbations

- Ions lost on their first poloidal transit ensures measurement of orbit deflection from a single pass through a perturbation

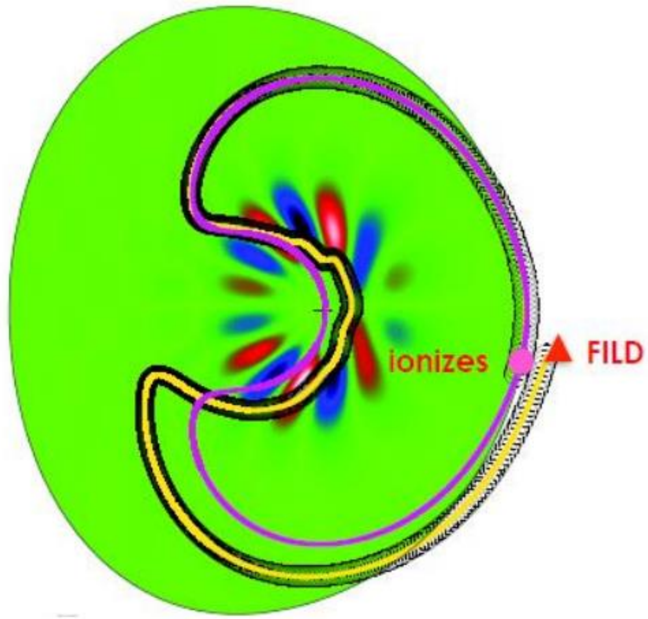

$$\xi = \frac{\Delta F}{F} L_i$$

*X Chen *et al* Nucl. Fusion **53** 123019 (2013)

First Radial Measurements of MHD-Induced Fast-Ion Losses

- MHD-induced FIL only observed when FILD is inserted

- Around mode local maximum:
  - ➢ Averaged FILD signal (F)
  - ➢ Convective FILD at mode frequency (ΔF)

- **Radial profiles of F and ΔF used to infer orbit displacement (ξ)**

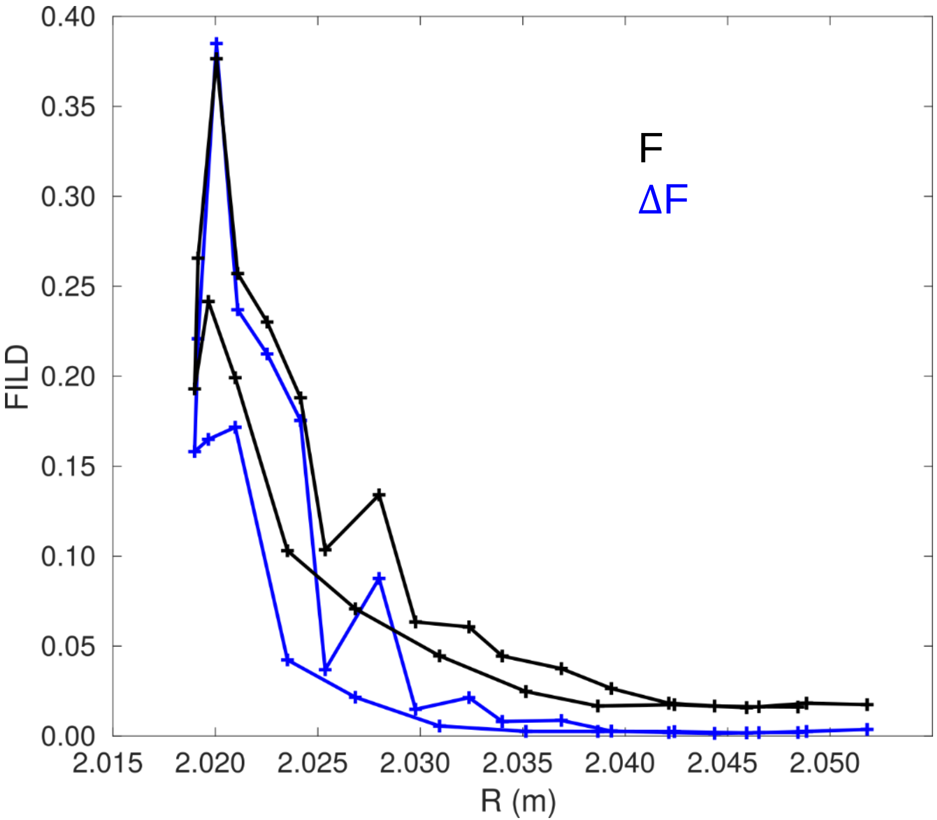

First Radial Measurements of MHD-Induced Fast-Ion Losses

- MHD-induced FIL only observed when FILD is inserted

- Around mode local maximum:
  - Averaged FILD signal (F)
  - Convective FILD at mode frequency (ΔF)

- Radial profiles of F and ΔF used to infer orbit displacement (ξ)

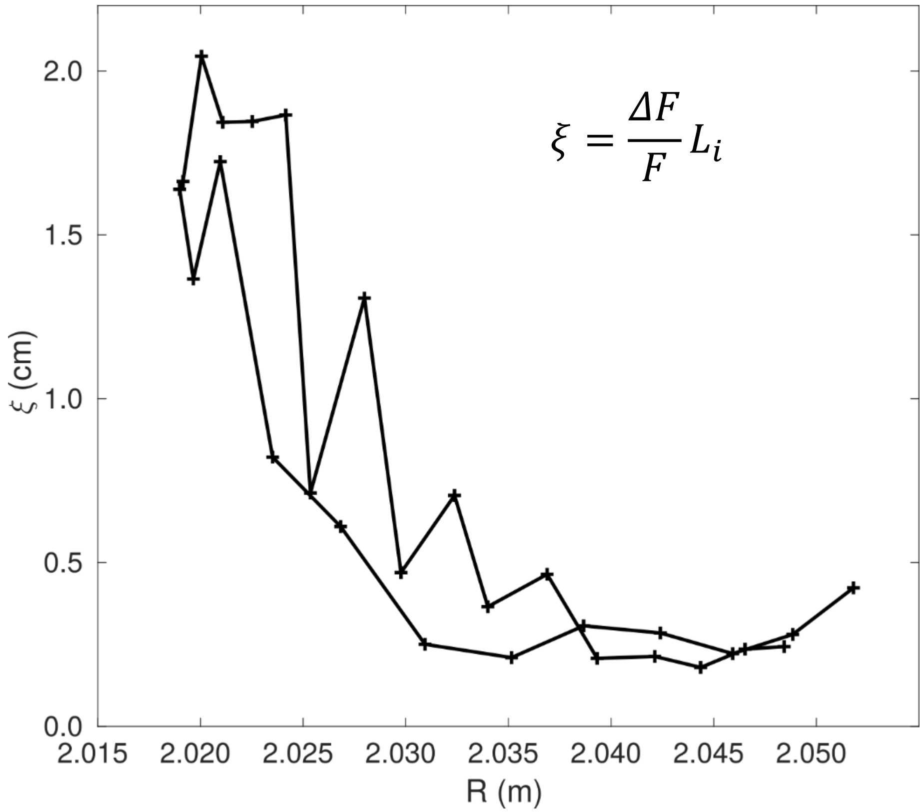

Orbit Kick Agrees with ECE Radial Measurement

- Orbit displacement at FILD location transformed to inner banana ρ_{pol} via measured orbits

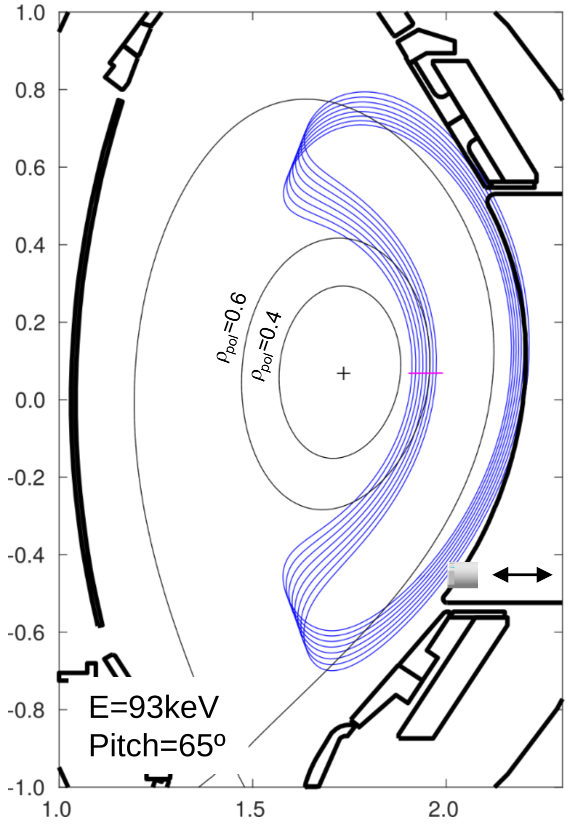

Orbit Kick Agrees with ECE Radial Measurement

- Orbit displacement at FILD location transformed to inner banana ρ_{pol} via measured orbits

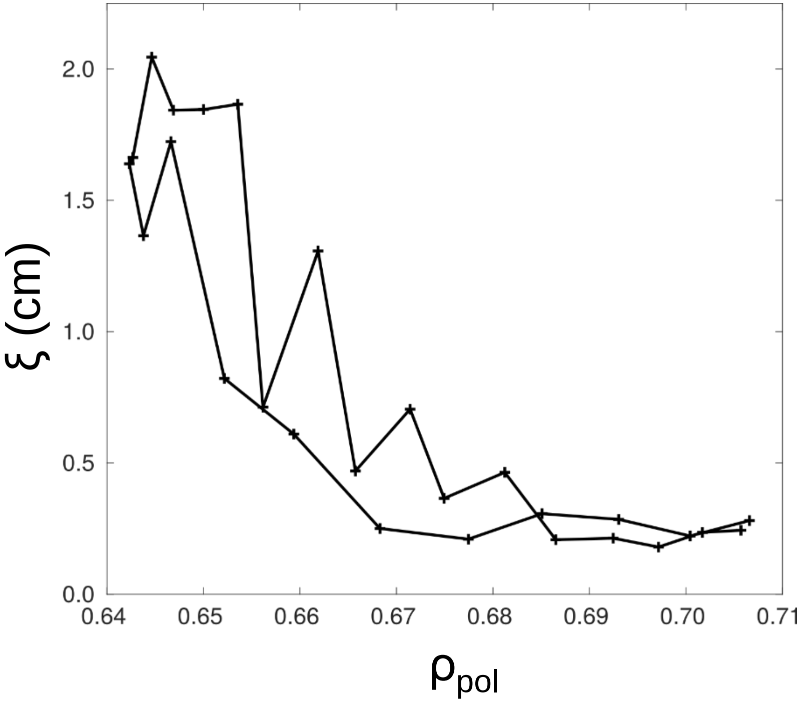

Orbit Kick Agrees with ECE Radial Measurement

- Orbit displacement at FILD location transformed to inner banana ρ_{pol} via measured orbits

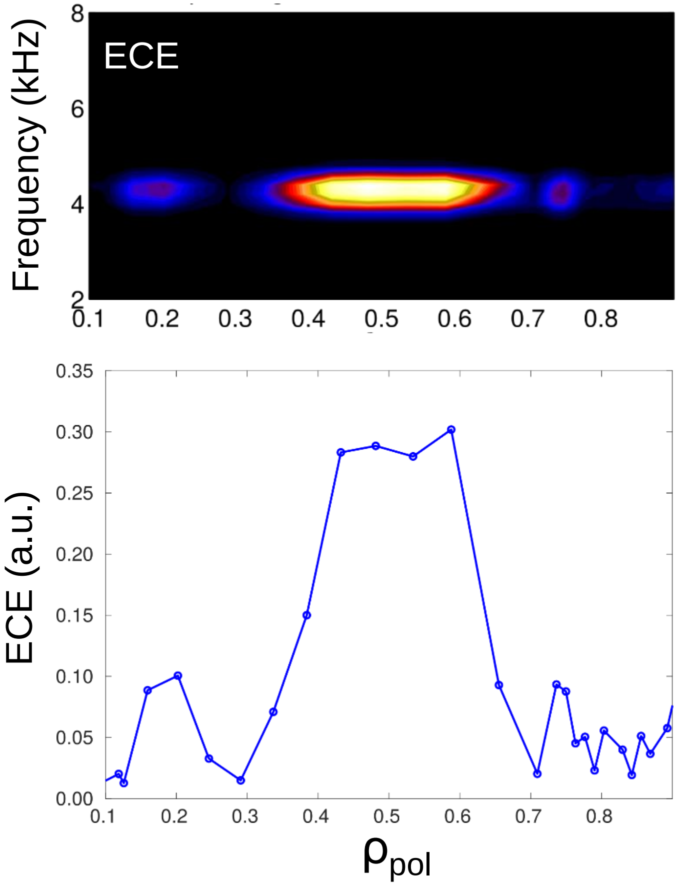

Orbit Kick Agrees with ECE Radial Measurement

- Orbit displacement at FILD location transformed to inner banana ρ_{pol} via measured orbits

- Despite limited radial range, FILD agrees with reconstructed ECE profile

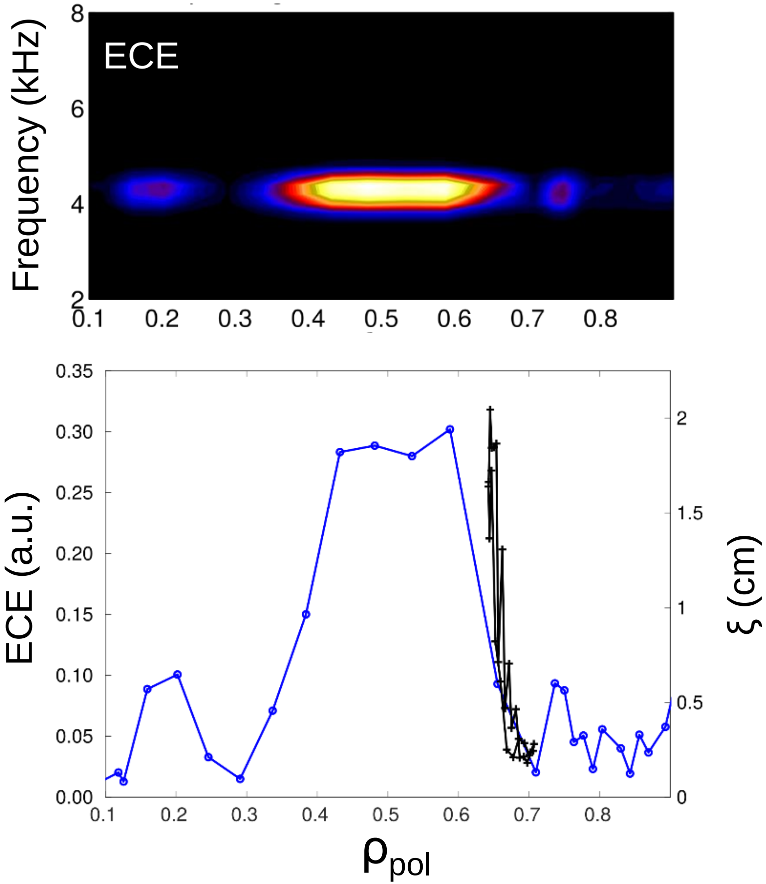

Orbit Kick Agrees with ECE Radial Measurement

- Orbit displacement at FILD location transformed to inner banana ρ_{pol} via measured orbits

- Despite limited radial range, FILD agrees with reconstructed ECE profile

- FILD limited range can be expanded by combining multiple orbits (APD pixels)

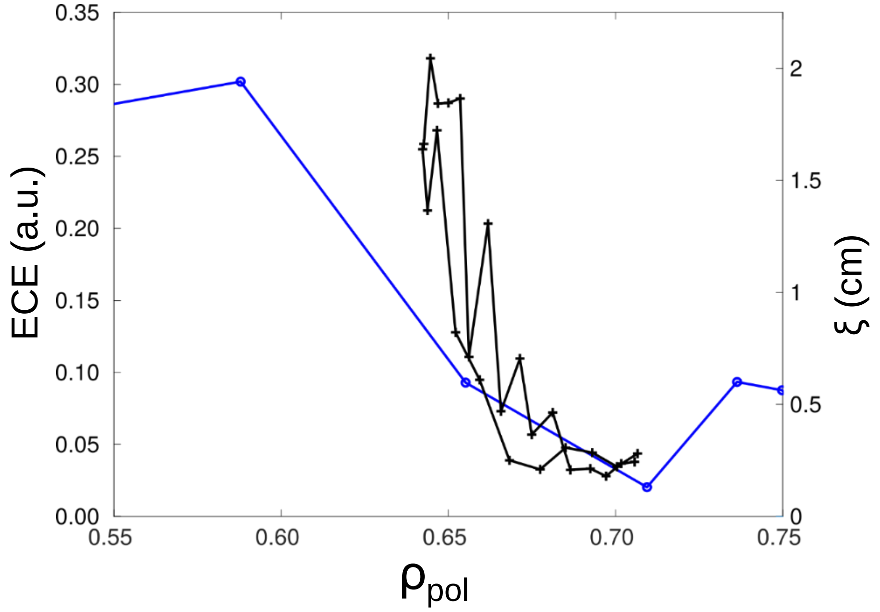

Outline

- Requirements of a Fast-Ion Loss Detector
- Scintillator-based Fast-Ion Loss Detector (FILD)
- Fast-Ion Losses Induced by:
  - Alfven Eigenmodes
  - Externally Applied Resonant Magnetic Perturbations
  - Edge Localized Modes (ELMs)
- Radial Profiles of Fast-Ion Losses
- **Synthetic FILD (FILDSIM)**

FILDSIM Code Simulates Expected Signal

J.Galdon-Quiroga *et al.*, PPCF 2018

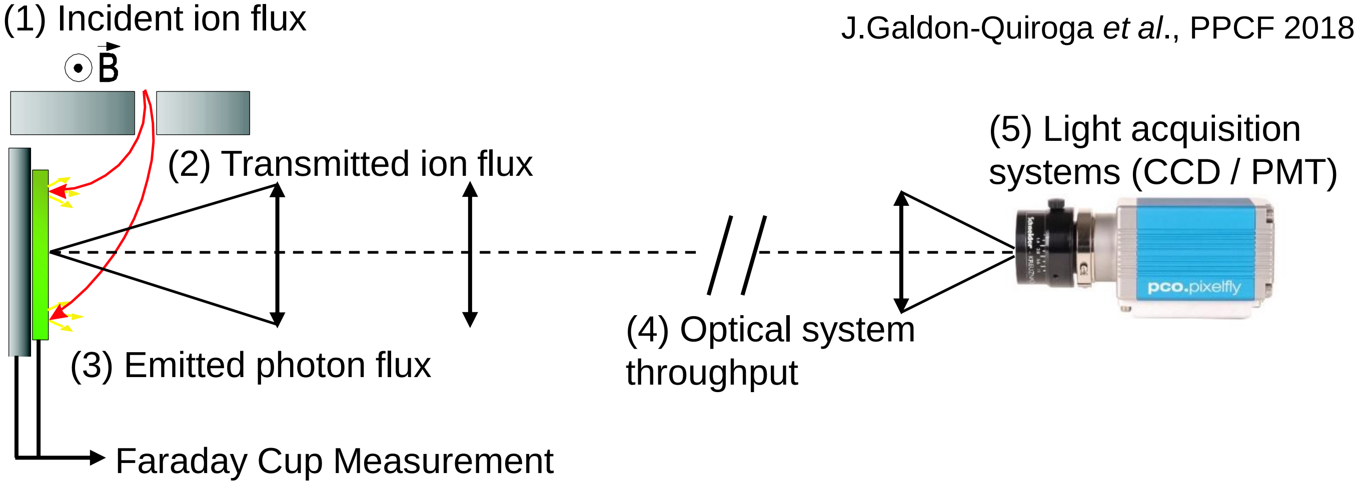

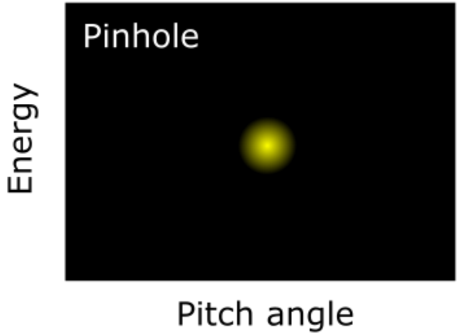

FILDSIM Code Simulates Expected Signal

J.Galdon-Quiroga *et al.*, PPCF 2018

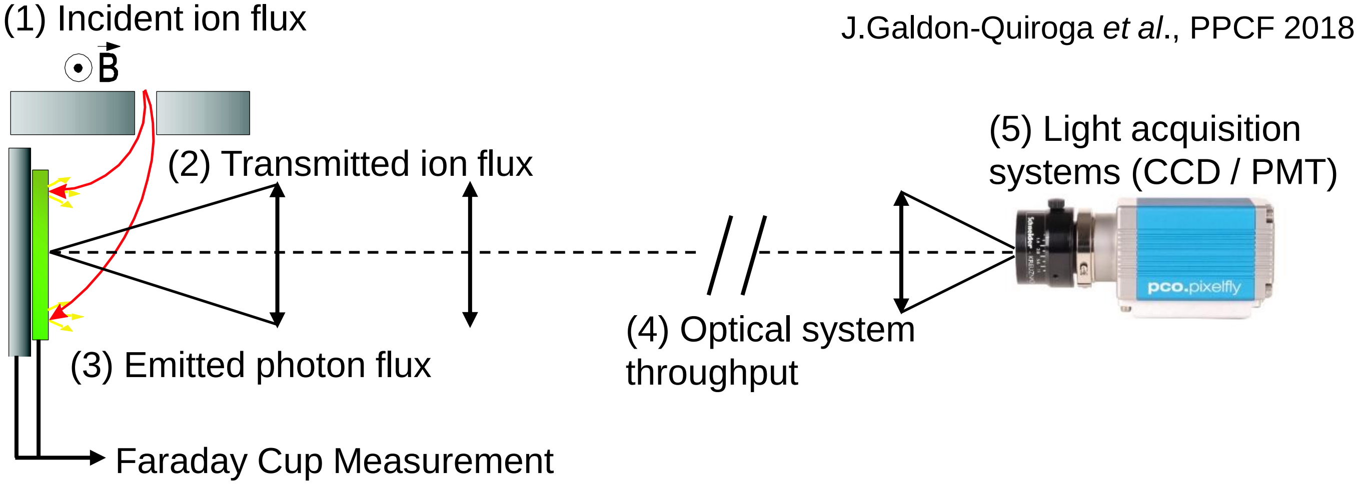

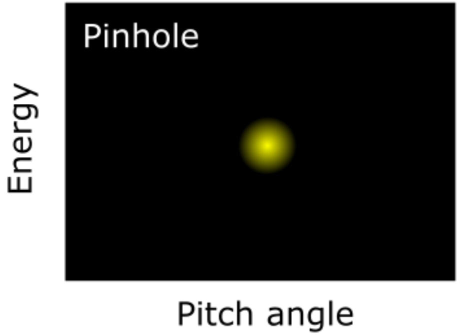

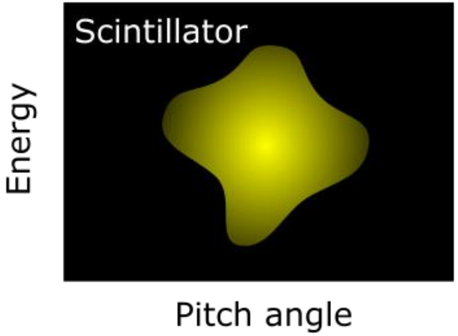

FILDSIM Code Simulates Expected Signal

J.Galdon-Quiroga *et al.*, PPCF 2018

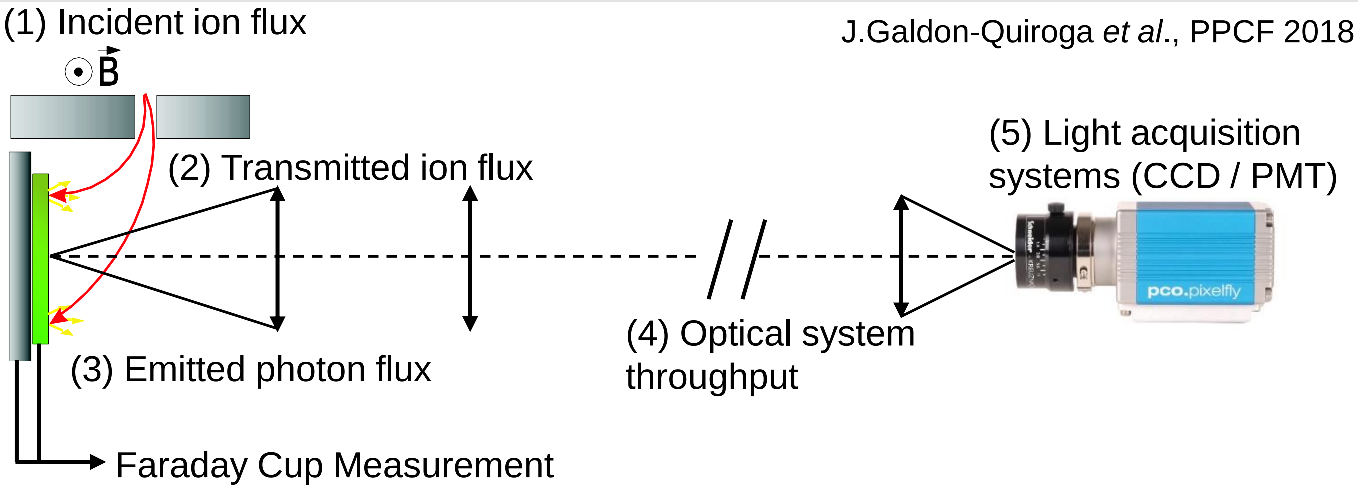

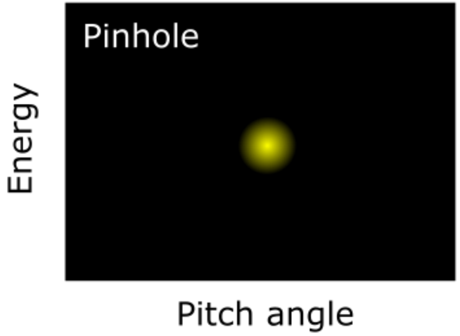

$$S_{ij} = \mathbf{W_{ijkl}} P_{kl}$$

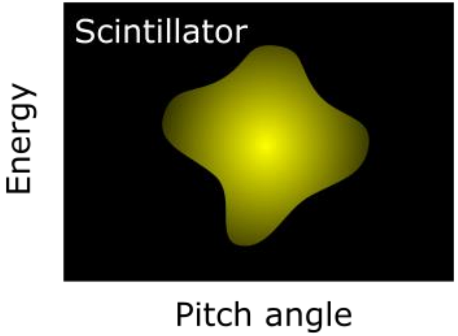

FILDSIM Code Simulates Expected Signal

J.Galdon-Quiroga *et al*., PPCF 2018

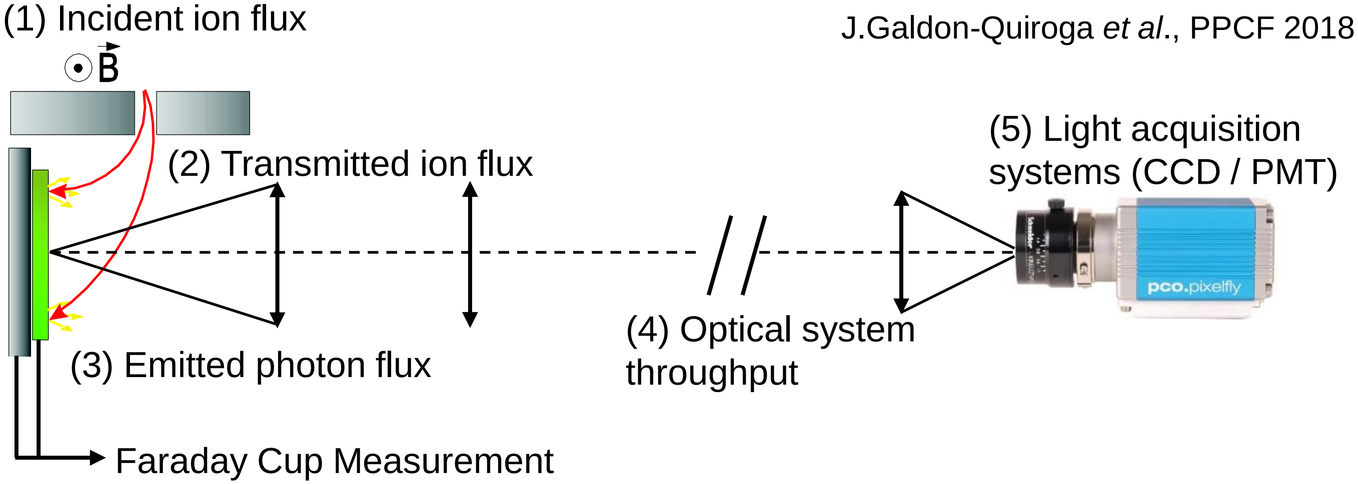

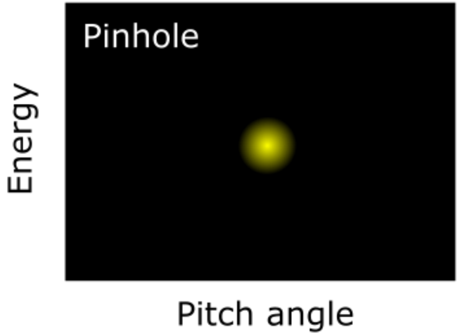

?

$$S_{ij} = \mathbf{W_{ijkl}} P_{kl}$$

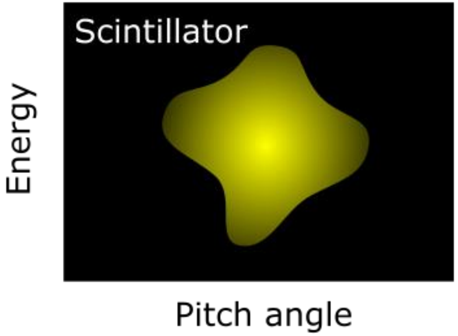

FILDSIM Code Simulates Expected Signal

J.Galdon-Quiroga *et al*., PPCF 2018

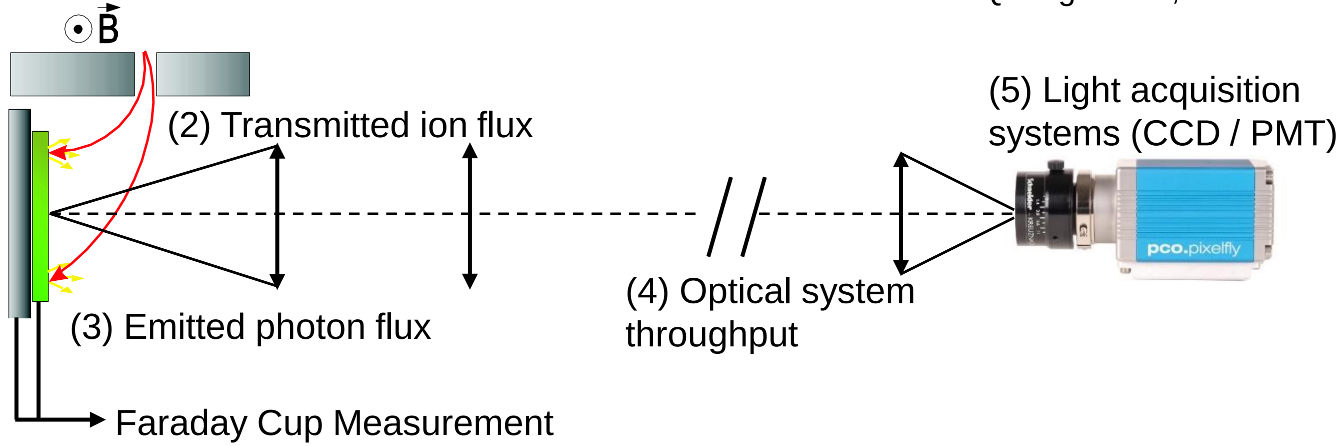

Synthetic FILD

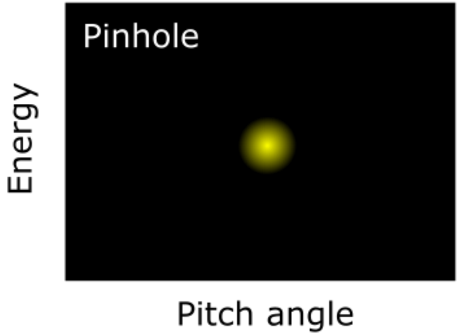

$$S_{ij} = \mathbf{W_{ijkl}} P_{kl}$$

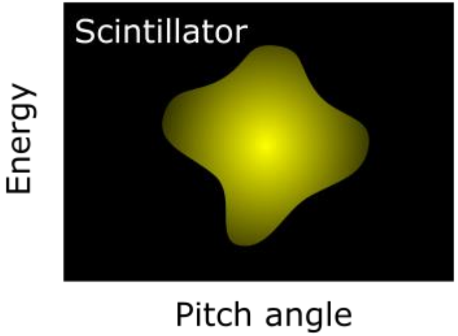

FILDSIM Code Simulates Expected Signal

J.Galdon-Quiroga *et al*., PPCF 2018

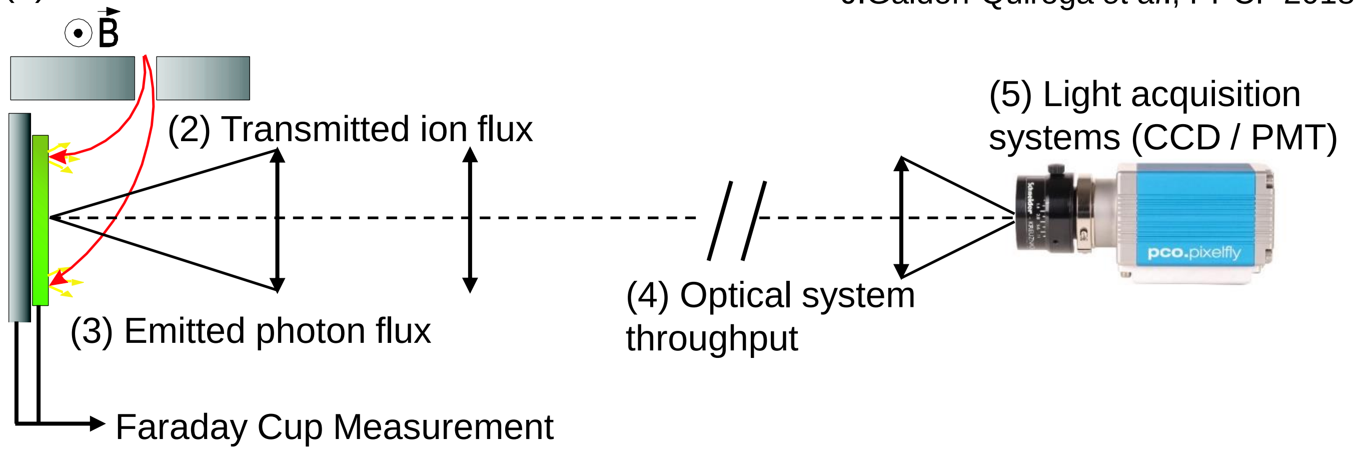

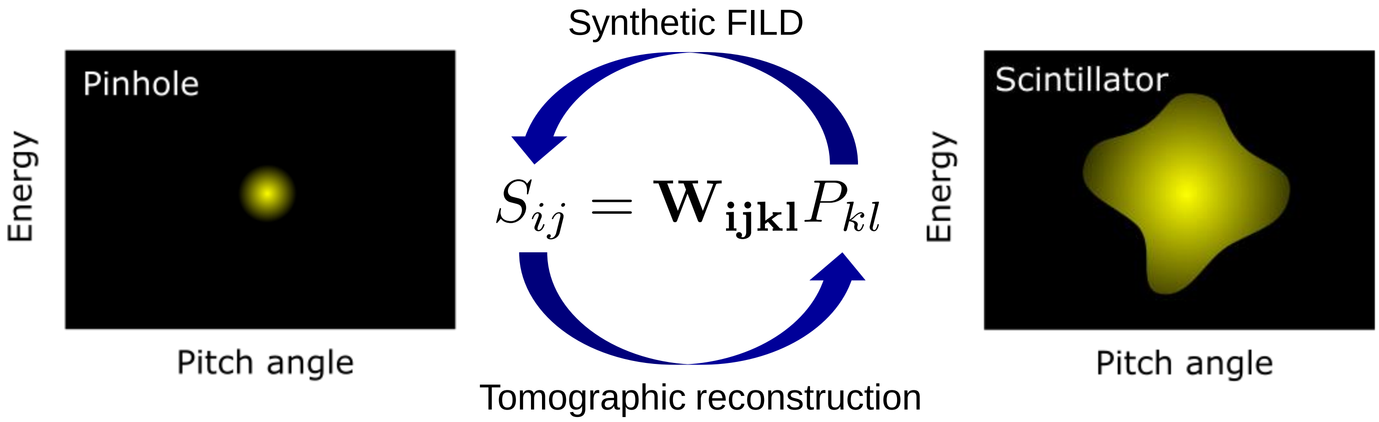

$$S_{ij} = \mathbf{W_{ijkl}} P_{kl}$$

FILDSIM Code Simulates Expected Signal

J.Galdon-Quiroga *et al*., PPCF 2018

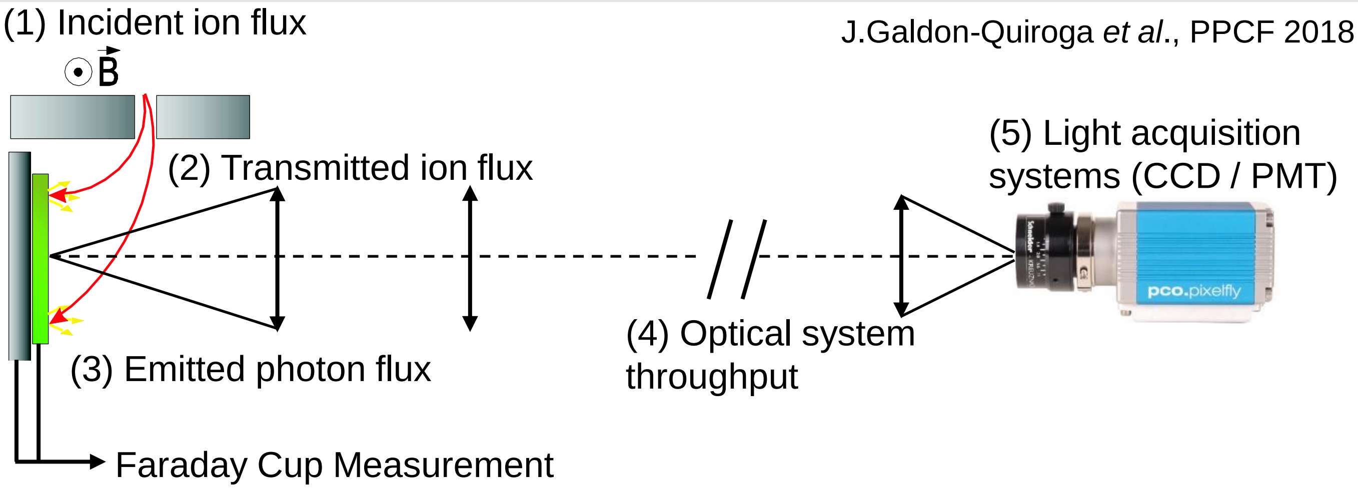

(1) $\boldsymbol{\Gamma_{ions}^{incident}}\quad [\boldsymbol{ions/s\cdot cm^2}]$

(2) $\boldsymbol{\Gamma_{ions}^{transmitted} = \Gamma_{ions}^{incident}\cdot A_{pinhole}\cdot f_{col}}\quad [\boldsymbol{ions/s}]$

(3) $\boldsymbol{\Gamma_{photons}^{emitted} = \Gamma_{ions}^{transmitted}\cdot Y_{scint}\cdot \frac{1}{4\pi}}\quad [\boldsymbol{photons/s\cdot sr}]$

(4) $\boldsymbol{\Gamma_{photons}^{transmitted} = \Gamma_{photons}^{emitted}\cdot \Omega\cdot T_{optics}}\ [\boldsymbol{photons/s}]$

FILDSIM Code Simulates Expected Signal

(1) Incident ion flux

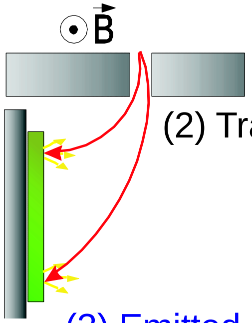

(2) Transmitted ion flux

(3) Emitted photon flux

$$\Gamma_s = \int \int w \cdot \Gamma_p \, d\Lambda \, d\rho$$

Γ_p: Incident ion flux at pinhole

Γ_s: Emitted photon flux by scintillator

FILDSIM Code Simulates Expected Signal

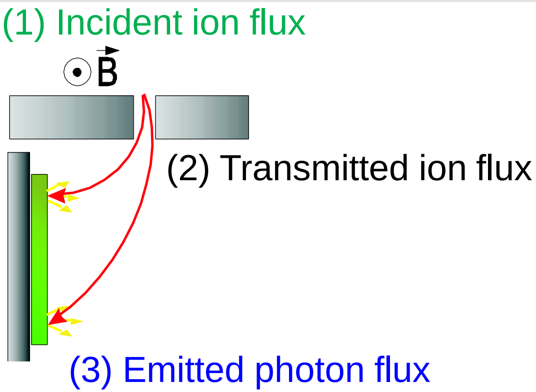

$$\Gamma_s = \int\int w \cdot \Gamma_p \, d\Lambda \, d\rho$$

Γ_p: Incident ion flux at pinhole

Γ_s: Emitted photon flux by scintillator

$w = T \cdot \epsilon$ – Weight function

T – Transfer function (accounts for detector resolution)

ϵ – Scintillator efficiency

$$T = \frac{f_{col}}{2\pi\sigma_\rho\sigma_\Lambda} \cdot exp\left[-\frac{(\rho'_L - \rho_L)^2}{2\sigma_\rho^2} - \frac{(\Lambda' - \Lambda)^2}{2\sigma_\Lambda^2}\right] \cdot \left[1 + \mathrm{erf}\left(\alpha_\rho \cdot \frac{(\rho'_L - \rho_L)}{\sqrt{2}\sigma_\rho}\right)\right]$$

FILDSIM Code Simulates Expected Signal

$$\Gamma_s = \int \int w \cdot \Gamma_p \, d\Lambda \, d\rho$$

Γ_p: Incident ion flux at pinhole

Γ_s: Emitted photon flux by scintillator

$w = T \cdot \epsilon$ – Weight function

T – Transfer function
(accounts for detector resolution)

ϵ – Scintillator efficiency

$$T = \frac{f_{col}}{2\pi\sigma_\rho\sigma_\Lambda} \cdot exp\left[-\frac{(\rho'_L - \rho_L)^2}{2\sigma_\rho^2} - \frac{(\Lambda' - \Lambda)^2}{2\sigma_\Lambda^2}\right] \cdot \left[1 + \mathrm{erf}\left(\alpha_\rho \cdot \frac{(\rho'_L - \rho_L)}{\sqrt{2}\sigma_\rho}\right)\right]$$

FILDSIM Code Simulates Expected Signal

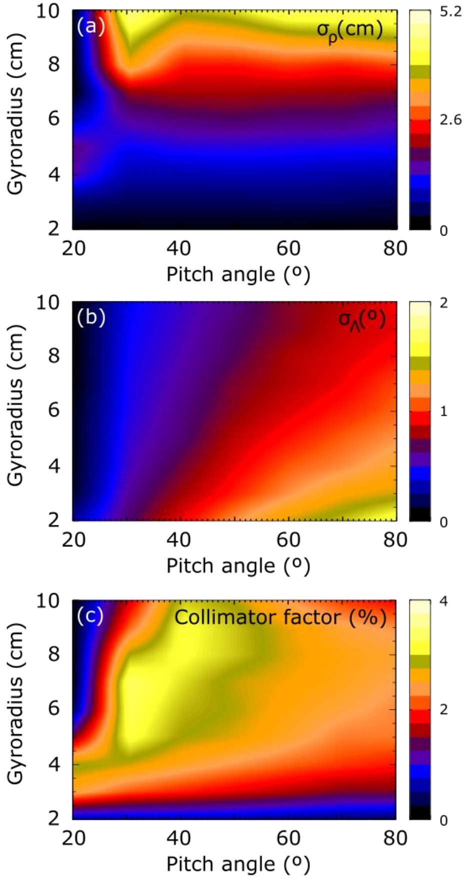

$$\Gamma_s = \int\int w \cdot \Gamma_p \, d\Lambda \, d\rho$$

Γ_p: Incident ion flux at pinhole

Γ_s: Emitted photon flux by scintillator

$w = T \cdot \epsilon$ — Weight function

T — Transfer function
(accounts for detector resolution)

ϵ — Scintillator efficiency

$$T = \frac{f_{col}}{2\pi\sigma_\rho\sigma_\Lambda} \cdot exp\left[-\frac{(\rho'_L - \rho_L)^2}{2\sigma_\rho^2} - \frac{(\Lambda' - \Lambda)^2}{2\sigma_\Lambda^2}\right] \cdot \left[1 + \mathrm{erf}\left(\alpha_\rho \cdot \frac{(\rho'_L - \rho_L)}{\sqrt{2}\sigma_\rho}\right)\right]$$

FILDSIM Code Simulates Expected Signal

$$\Gamma_s = \int\int w \cdot \Gamma_p \, d\Lambda \, d\rho$$

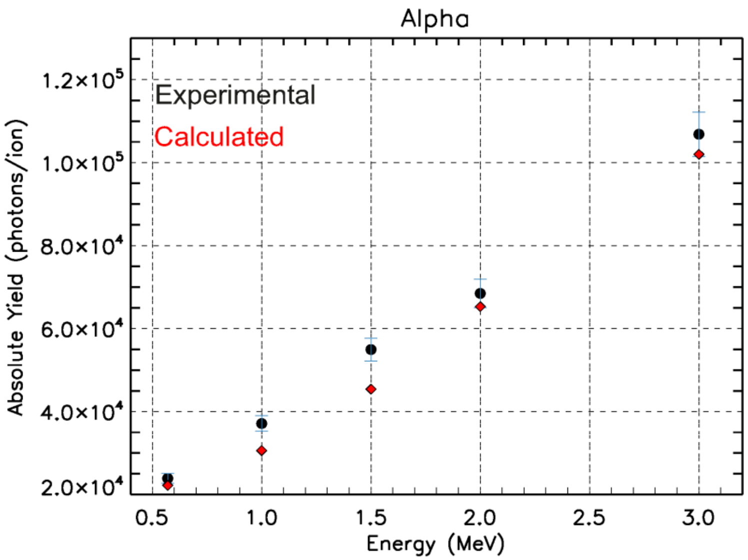

Γ_p: Incident ion flux at pinhole

Γ_s: Emitted photon flux by scintillator

$w = T \cdot \epsilon$ – Weight function

T – Transfer function (accounts for detector resolution)

ϵ – **Scintillator efficiency**

$$T = \frac{f_{col}}{2\pi\sigma_\rho\sigma_\Lambda} \cdot exp\left[-\frac{(\rho'_L - \rho_L)^2}{2\sigma_\rho^2} - \frac{(\Lambda' - \Lambda)^2}{2\sigma_\Lambda^2}\right] \cdot \left[1 + \mathrm{erf}\left(\alpha_\rho \cdot \frac{(\rho'_L - \rho_L)}{\sqrt{2}\sigma_\rho}\right)\right]$$

Absolute Flux Obtained from FILD Calibration

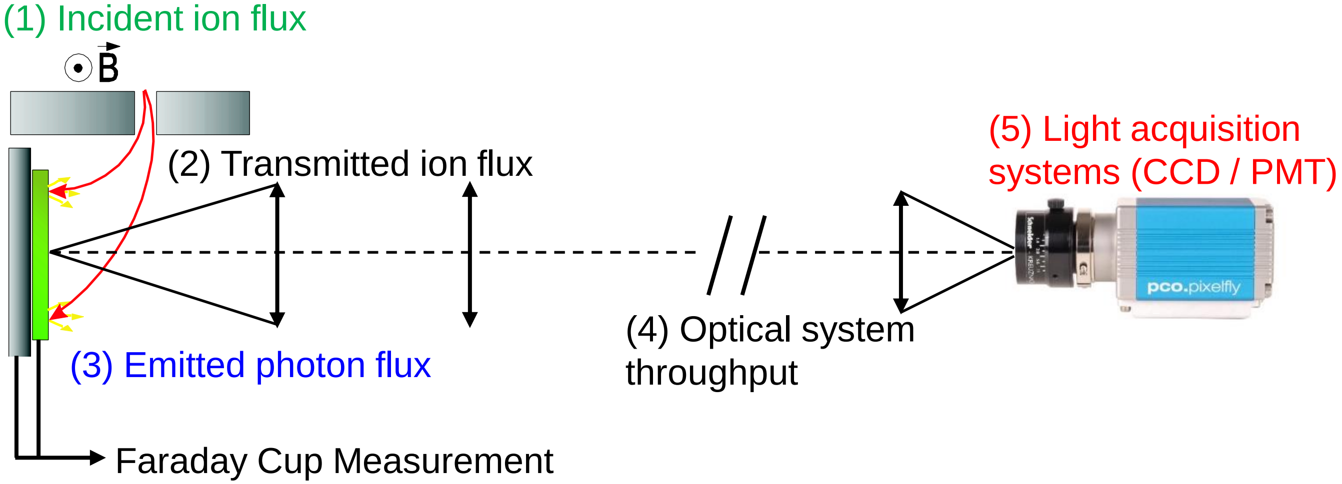

$$\Gamma_s = \int \int R \cdot C \cdot I \, dp \, dq$$

Γ_s: Emitted photon flux by scintillator

I: Pixel intensity

R – Mapping function
pixel space > velocity space

C – Calibration function

$$C_{pq} = \frac{1}{A_P \cdot \Delta t \cdot \xi_{pq}} = \frac{\Phi_{IS} \cdot S_\Omega \cdot \Delta t_{IS}}{A_P \cdot \Delta t \cdot I_{pq}^{IS}},$$

Absolute Flux Obtained from FILD Calibration

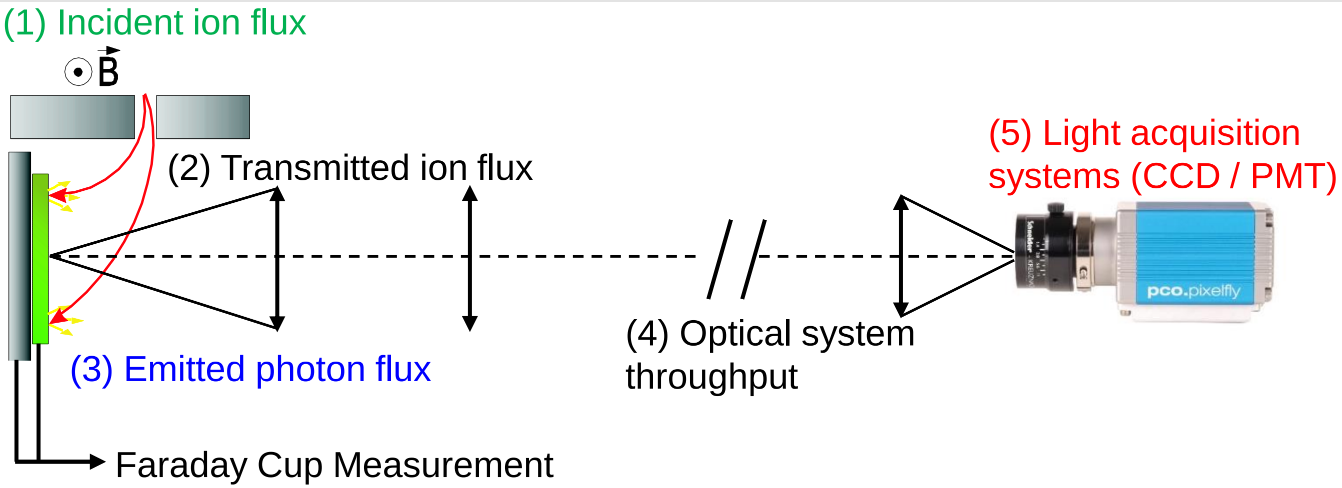

ALL in one

$$\boxed{\int\int R \cdot C \cdot I \, dp \, dq = \int\int T \cdot \epsilon \cdot \Gamma_p \, d\Lambda \, d\rho}$$

FILDSIM Has Been Widely Used to Design FILD Systems…

ITER FILD design includes estimated FC signal with nuclear background (gammas + charge particles generated in scintillator itself)

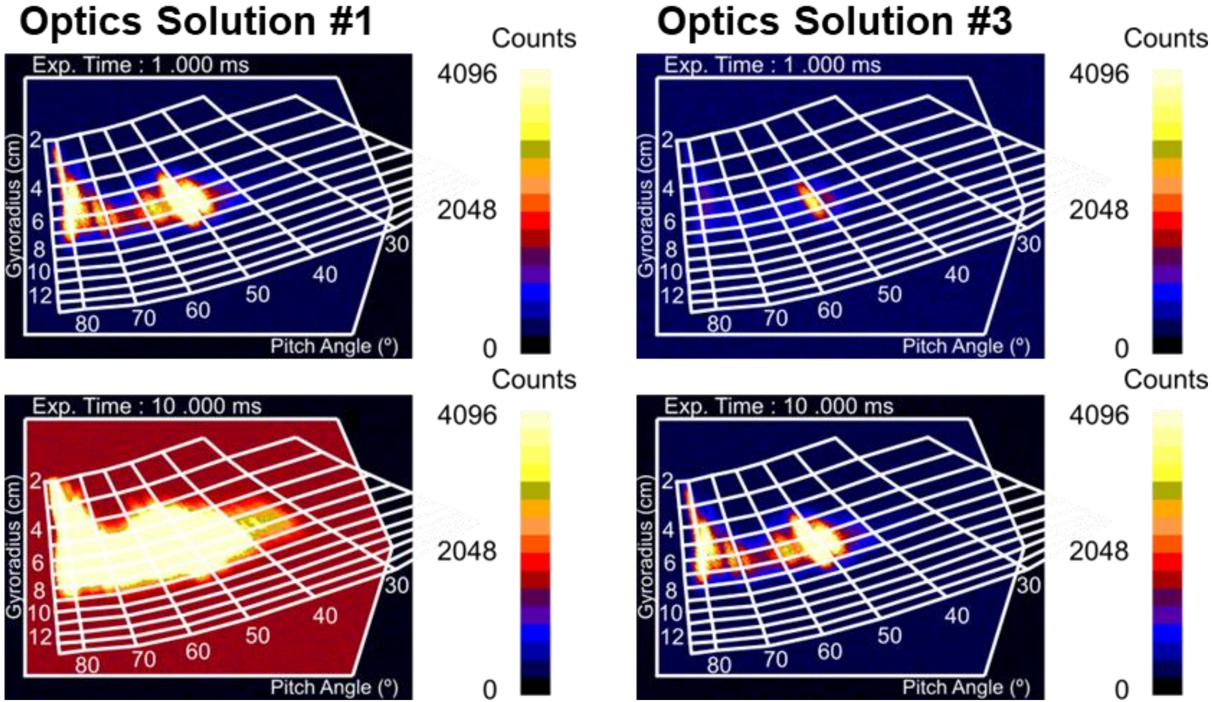

…Characterise FILD Response…

FILDSIM is routinely used to obtain absolute fluxes of fast-ion losses

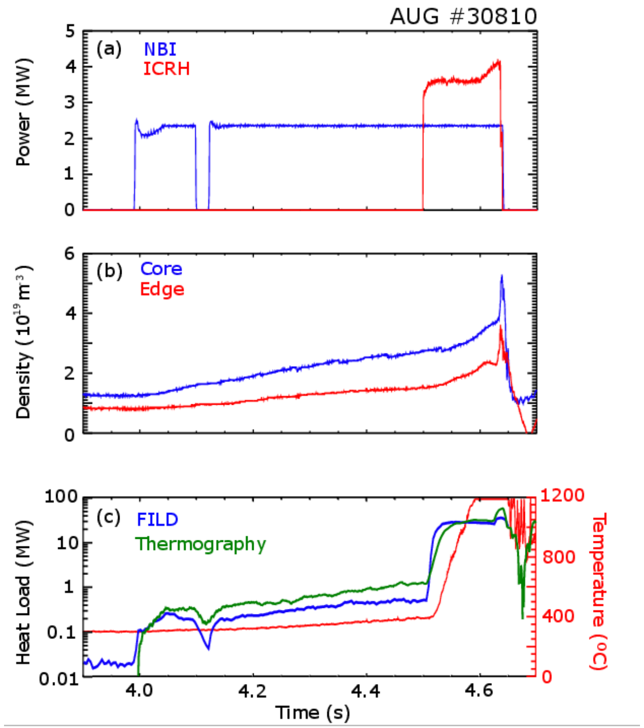

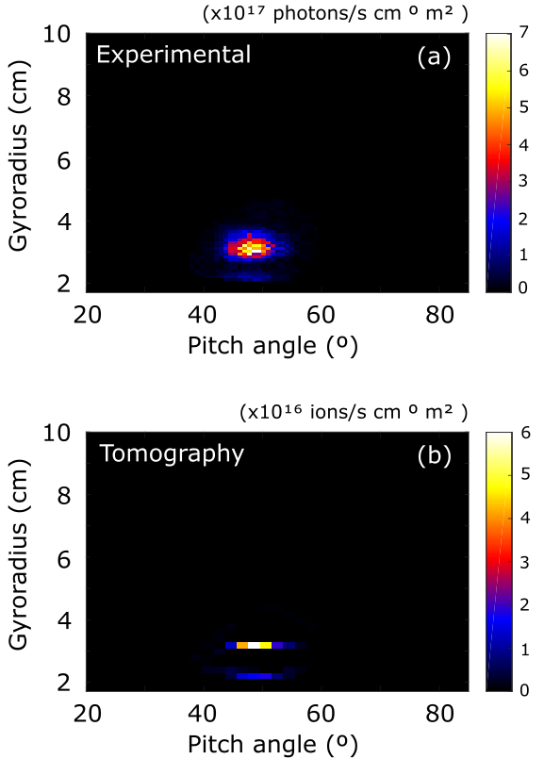

Observation of beam ions acceleration during ELMs*

- Main and half energy components are **well matched**

- **Well localized energy distribution** rather than a large spread

- Recovered synthetic scintillator signal in good agreement with experimental measurement

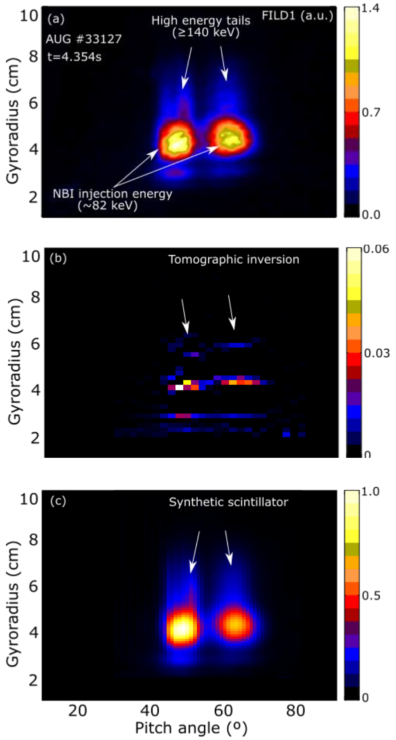

*J.Galdon-Quiroga et al., PRL (2018)

Final Remarks

- Fast-ions are very well confined in tokamaks in the absence of MHD perturbations
- However, subject to transport / loss by a large spectrum of MHD perturbations (internal + external)
- At present, there is no technique capable of covering full phase-space of escaping ions
- Combination of diagnostics and modelling tools give confident predictions towards future devices

Synthetic ITER FILD measurement:
Alpha particles losses induced by n=4 RMP

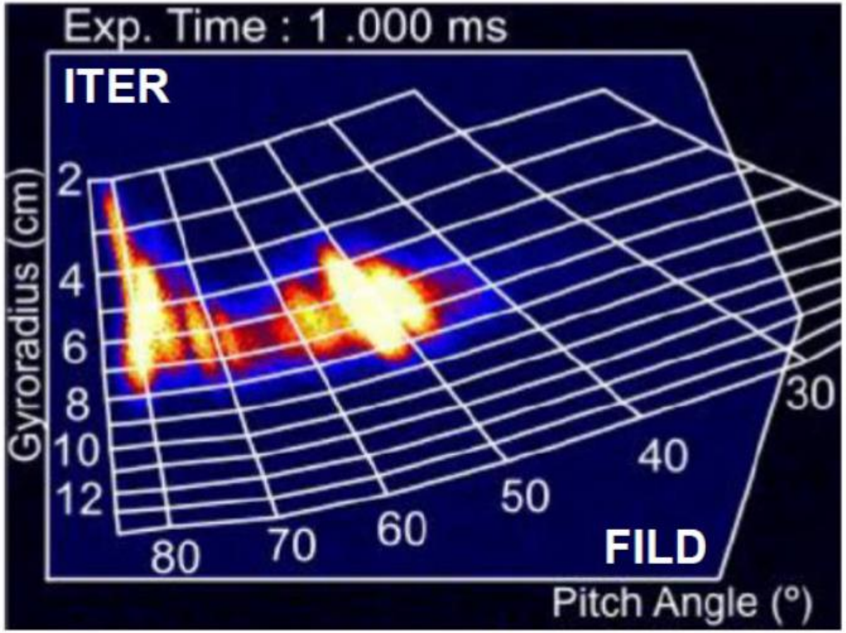

M. Garcia-Munoz *et al.*, Rev. Sci. Instrum. **87**, 11D829 (2016)